ÇUKUROVA UNIVERSITY
INSTITUTE OF NATURAL AND APPLIED SCIENCES

MSc THESIS

Altan ÇETİNGÖZ

ENERGY ANALYSIS OF SOLAR-POWERED ABSORPTION COOLING SYSTEM IN MERSIN

DEPARTMENT OF MECHANICAL ENGINEERING

ADANA, 2015

ÇUKUROVA UNIVERSITY
INSTITUTE OF NATURAL AND APPLIED SCIENCES

ENERGY ANALYSIS OF SOLAR-POWERED ABSORPTION COOLING SYSTEM IN MERSIN

Altan ÇETİNGÖZ

MSc THESIS

DEPARTMENT OF MECHANICAL ENGINEERING

We certify that the thesis titled above was reviewed and approved for the award of degree of the Master of Science by the board of jury on 09/03/2015.

…….....	……	…….....
Prof. Dr. Beşir ŞAHİN	Prof. Dr. Hüseyin AKILLI	Assoc. Prof. Dr. Mehmet BİLGİLİ
SUPERVISOR	MEMBER	MEMBER

This MSc Thesis is written at the Department of Institute of Natural And Applied Sciences of Çukurova University.
Registration Number:

Prof. Dr. Mustafa GÖK
Director
Institute of Natural and Applied Sciences

ABSTRACT

MSc THESIS

ENERGY ANALYSIS OF SOLAR-POWERED ABSORPTION COOLING SYSTEM IN MERSIN

Altan ÇETİNGÖZ

ÇUKUROVA UNIVERSITY
INSTITUTE OF NATURAL AND APPLIED SCIENCES
DEPARTMENT OF MECHANICAL ENGINEERING

Supervisor : Prof. Dr. Beşir ŞAHİN

Year: 2015, Pages: 79

Jury : Prof. Dr. Hüseyin AKILLI
: Assoc. Prof. Dr. Mehmet BİLGİLİ

In this study, solar-powered absorption cooling system located in the province of Mersin was analyzed using hourly atmospheric temperature and solar radiation data. Ammonia-water as refrigerant-absorbent pairs and evacuated tube collector were chosen for the design of solar-powered absorption cooling system. Required solar collector areas were calculated for heat loads of the refrigerated space. According to obtained results, Coefficient of Performance (COP) values were also changed for the 23rd day of chosen months. The maximum COP values were observed in May, while the lowest values were seen in July and August. The maximum solar radiation was observed on 23 June at 01:00 pm. At this time, COP was calculated as 0.786, while solar radiation was 0.878 kW/m^2. The optimum collector area required for cooling is determined as 50 m^2 for a refrigerated space of 30 m^2.

Key Words: Absorption cooling, COP, evacuated tube collector, solar radiation, thermal energy

ÖZ

YÜKSEK LİSANS TEZİ

MERSİN'DE YERALAN GÜNEŞ ENERJİLİ ABSORBSİYONLU SOĞUTMA SİSTEMİNİN ENERJİ ANALİZİ

Altan ÇETİNGÖZ

ÇUKUROVA ÜNİVERSİTESİ
FEN BİLİMLERİ ENSTİTÜSÜ
MAKİNA MÜHENDİSLİĞİ ANABİLİM DALI

Danışman :Prof. Dr. Beşir ŞAHİN
Yıl: 2015, Sayfa: 79
Jüri :Prof. Dr. Hüseyin AKILLI
:Doç. Dr. Mehmet BİLGİLİ

Bu çalışmada Mersin ilinde yer alan soğutma alanında kullanılacak güneş enerjili absorbsiyonlu soğutma sistemi saatlik atmosfer sıcaklığı ve güneş ışınımı verileri kullanılarak analiz edilmiştir. Vakum tüplü güneş kolektörü ve amonyak-su soğutucu çifti seçilerek güneş enerjili absorbsiyonlu soğutma sistemi tasarlanmıştır. Soğutma alanının ısıl yükleri dikkate alınarak sistem için gerekli güneş kolektörü alanı hesaplanmıştır. Elde edilen sonuçlara göre COP değerleri her seçilen ayın 23'üncü günü için değiştiği belirlenmiştir. En yüksek COP değerleri Mayıs, en düşük COP değerleri Temmuz ve Ağustos aylarında gözlemlenmiştir. En yüksek güneş ışınım değeri Haziran ayının 23'ünde öğleden sonra 01:00'da gözlemlenmiştir. Bu değer 0.878 kW/m^2 iken COP 0.786 olarak hesaplanmıştır. Soğutma için gerekli optimum kolektör alanı 30 m^2'lik soğutulacak bir alan için 50 m^2 olarak belirlenmiştir.

Anahtar Kelimeler: Absorbsiyonlu soğutma, COP, Vakum tüplü kolektör, Güneş ışınımı, Isıl enerji

ACKNOWLEDGEMENTS

I would like to thank to my supervisor Prof. Dr. Beşir ŞAHİN for his guidance and help throughout the thesis study. I also owe my deepest gratitude for his everlasting patience and his positive approach during the whole study.

I would like to thank Assoc. Prof. Dr. Mehmet BİLGİLİ for his technical support, professional advice and guidance from initial to final level enabled me to develop an understanding of the subject. I am grateful to my committee member Prof. Dr. Hüseyin AKILLI for his expert comments.

I would like to thank my friends Kemal Can KEVSER for his suggestions and İbrahim Çağlar AĞCA for his support.

And finally, special thank to my mother Halime ÇETİNGÖZ, my sister Gökçe ÇETİNGÖZ AKBAY and my wife Özge SARAÇ ÇETİNGÖZ for their endless support. My deepest appreciation goes to my family members for their love, sharing, understanding, warm attitude and endless support.

This thesis is dedicated to my father Ferit ÇETİNGÖZ with all my heart.

CONTENTS **PAGE**

LIST OF TABLES **PAGE**

LIST OF FİGURES **PAGE**

NOMENCLATURE

CO_2 **:** carbon dioxide

COP **:** coefficient of performance

IC **:** ideal cooling

IH **:** ideal heating

T **:** temperature

LiBr **:** lithium bromide

$\dot{m}$ **:** mass flow rate

x **:** mass concentration

NH_3 **:** ammonia

Q **:** heat transfer

W **:** pump work

G **:** generator

C **:** condenser

E **:** evaporator

A **:** absorber

h **:** enthalpy

f **:** mass flow ratio

q **:** heat dissipated per unit mass

Q_{sol} **:** solar radiation received with the solar collector

$Q_{sol\text{-}gen}$ **:** heat transferred from solar collector to generator

η **:** thermal efficiency of solar collector

τ **:** coefficient of the transmission

α **:** coefficient of the absorption

U **:** overall heat transfer coefficient

F **:** solar-collector efficiency factor

l **:** liter

I **:** solar radiation

D/D **:** degree day

HDD **:** heating degree days

CDD **:** cooling degree days

1. INTRODUCTION

1.1. Human Comfort and Air Conditioning

Humanity has been searching for comfort since the world life began. Air conditioning and refrigeration systems have an important part in the modern human life. For example, fire is the first air conditioning application in history.

Air conditioning applications such as heating and cooling systems have been developed rapidly in the recent years. Cooling systems started to play an important role in human life with the advancement of technology. The need for cooling in hot climates and especially during the summer months is more emphasized nowadays.

The annual average daily temperature is expected to increase by 2 °C to 4 °C until 2080. The size of air conditioned floor space in summer exceeded 150 million m^2 in 2000 in Europe, while it was 30 million m^2 in 1980 (Agyenim et al., 2010).

Increases in air conditioning applications in conjunction with rising living and working comfort have a negative impact on energy consumption and environment. According to Bermejo (2010), the energy consumption for heating is expected to be stabilized after 2030. Energy consumption for cooling increases rapidly along with global warming.

In general, nuclear energy and fossil fuels (coal, oil, natural gas) as well as renewable energy sources are used for electricity production. Steam power which enabled the industrial revolution made it possible to produce electricity with thermal applications. Easily accessible fossil fuels were used in the thermal power plants for many years.

The consumption of fossil fuels increases proportionally with an increase of the world energy demand. Contrary to the popular belief in many years, fossil fuels are not inexhaustible. Moreover, it became even more important to restrict fossil fuel consumption with CO_2 emissions having reached of dangerous level.

Fossil energy sources are being depleted rapidly because of raising worldwide energy consumption. Therefore, efficient use of energy sources has become an important issue due to the limited sources of fossil fuels (Agyenim, 2010). Existing

fossil fuel-based energy systems have a large share in the formation of the humanitarian, environmental and economic crisis (Bermejo, 2010). Although there have been several research works performed on the optimizations of energy systems these energy systems still have a low performance coefficient. It is still necessary to conduct researches in order to improve design parameters of energy systems further.

The system considered in this investigation works with fluids such as water and ammonia for preserving environment. These working fluids have zero ozone depletion potential in accordance with the Montreal Protocol and zero global warming potential in accordance with the Kyoto Protocol's (Ahachad, 2005). Compression cycles working with photovoltaic energy are expensive and cannot give the desired yield in the developing countries. Using solar energy in thermal applications is a more efficient alternative in solar sorption cooling. The solar energy can be used directly by the vapor compression cycle without the need of any energy conversion (Ahachad, 2005). The demand for absorption refrigeration systems increases rapidly because they consume low level of energy. In summer, solar absorption cooling systems become both economic and ecological applications by combining the need for cooling of buildings with a high rate of availability of solar energy (Ali, 2008). The reason of solar cooling system being a major study subject is to use solar energy intensively in the period of cooling load peaks. Solar cooling systems are remarkable alternatives for conventional air conditioning systems. The solar energy is used as an energy source without any extra. It is a good example for the coordination of the need for cooling and energy supply (Marc, 2010). There is a parallelism between the need for cooling during the day and the supply of solar energy. That is to say cooling demand and availability of solar energy are high at the same time (Ersoy, 2007). The annual average solar-radiation is 3.6 kWh/m^2day and the total annual radiation period is 2610 h in Turkey (Ali, 2008). Around noon time in the southern parts of Turkey, the highest level of solar radiation can be 900 W/m^2 (Ersoy, 2007). Turkey is located in the "sun belt" with its geographical location (36 °-42 ° north latitude). So, solar energy applications are possible in the majority of Turkey.

Absorption machines operate with thermal energy. They don't need a high input power. Therefore, they can be used in places where the energy is expensive or inaccessible. At the same time, they provide reliable and economical cooling application using existing waste, geothermal or solar heat (Florides, 2002). Olesen (2012) reports that during the summer months, the necessary temperatures for human comfort are in between 23.5 °C and 25.5 °C. Taking the ambient temperature of 24 °C is a common practice in studying the air conditioning applications. Therefore, cooling application is a requirement when the ambient temperature is higher than 24 °C. Solar-powered absorption cooling system is an alternative cooling method that is largely thermal driven and requires little external work (Atmaca, 2003).

1.2. Solar Energy

Solar energy is used for heating of buildings, demand of hot water, electricity generation, thermal systems and solar cells. The production of electricity from solar energy has become inevitably important. Solar cells can be used economically in remote areas where there is no electricity network. Using of solar cells in widespread area depends on lowering costs. Therefore, they are used on signaling and in rural areas if there is no electricity network (Çolak et al., 2008). According to Atlas of Turkey's Solar Energy Potential (GEPA) prepared from General Directorate of Renewable Energy, the annual sunshine time is 2,737 hours (daily total is 7.5 hours) and the total annual solar energy is 1,527 kWh/m²year (daily total is 4.2 kWh/m).

In Turkey, according to Ministry of Energy and Natural Resources the total installed solar collector area was calculated as approximately 18,640,000 m^2 by the end of 2012. Annual production of flat plate solar collector is 1,164,000 m² and vacuum tube collector has been calculated as 57,600 m². Fifty percent of produced flat collectors and all produced vacuum tube collectors are used in Turkey. In 2012, produced heat energy by solar collectors was approximately 768,000 tonnes oil equivalent (TOE). The produced thermal energy was used in residents as 500,000 TOE and thermal energy of 268,000 TOE was used in industry. In Turkey, established photovoltaic solar electric systems amounted to 3.5 MW installed power

that used to satisfaction small power of public institutions and research purposes (Ministry of Energy and Natural Resources).

Efficiently use of energy and the share in developing and developed countries depend on sufficient of energy resources. Until the middle of the twenty-first century, a large amount of the world's energy demand may be obtained from fossil fuels (Çolak et al., 2008). Electric necessity of the world is produced by petroleum-derived fuels. Figure 1.1 indicates the energy sources for electricity production (International Energy Agency, 2014). According to (International Energy Agency, 2014), presently, a large amount of the world's electrical energy demands are generated from the fossil fuels; the share of fossil fuels is about 50% on electricity production. On the other hand renewable energy sources have presently 21% share. In general, energy production must be increased in order to compensate the world's energy consumption preserving the continuation of industrial development and growth of global economy. Since there are no fossil fuel sources in every region of the world, political and economic problems on fossil fuel producers affect the whole world.

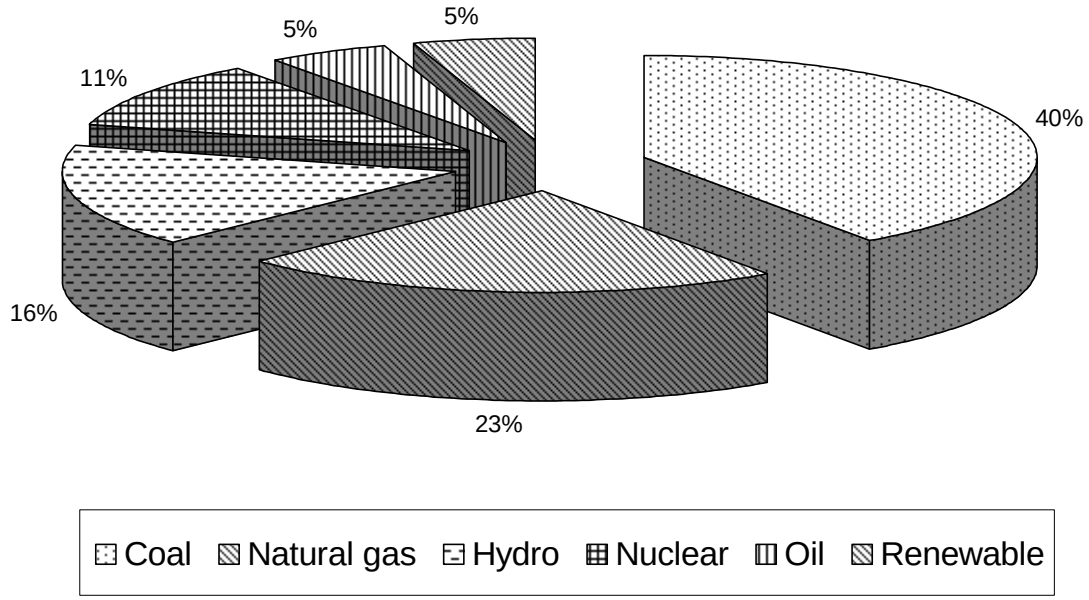

Figure 1.1: Production of electricity based on the energy source all over the world in 2012 (International Energy Agency, 2014)

Also serious environmental pollution problems occur during the electricity production with today's technology using the traditional energy sources such as fossil fuels. Researches on the renewable energy systems increases rapidly due the shortage of fossil fuels in the future, cost of fossil fuels and serious environmental pollution problems caused by these sources fossil fuels.

The world's energy consumption increased 57% as more than expected in the last twenty years. Generated energy will not cover the amount of demand of energy in the world during the next 20 or 30 years (Çolak et al., 2008).

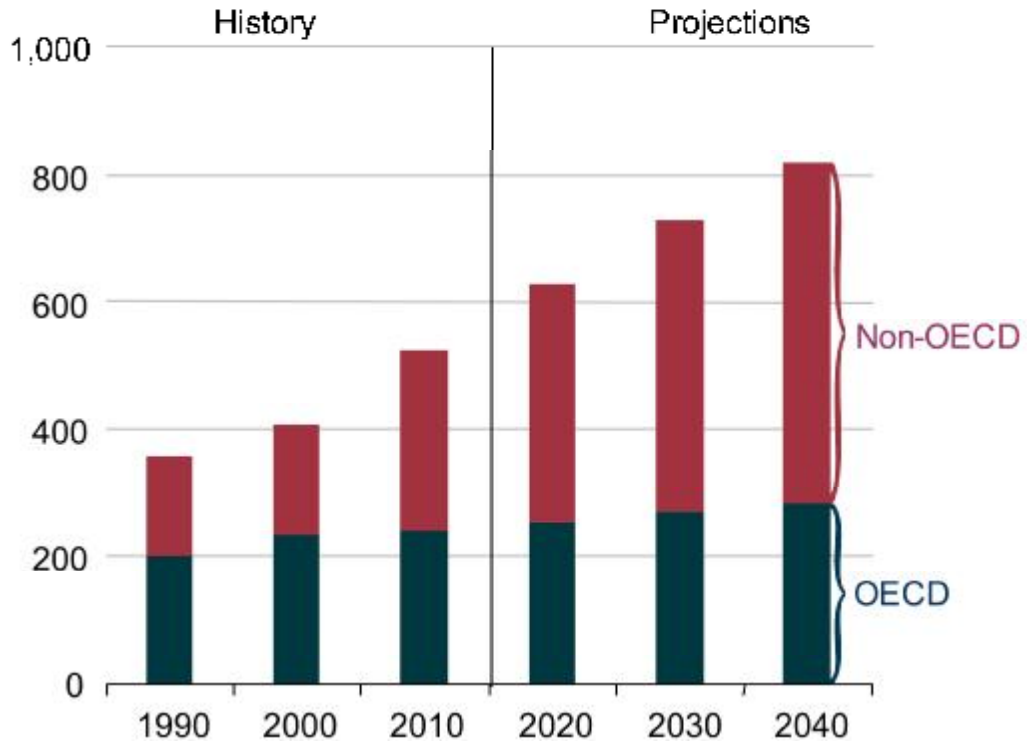

Fig. 1.2: World energy consumption, 1990-2040 (quadrillion Btu) (U.S. Energy Information Administration, 2013)

World energy consumption is observed in Figure 1.2 (U.S. Energy Information Administration, 2013). The increase by an average of 3.6 percent per year is expected on the world's real gross domestic product (GDP, expressed in purchasing power parity terms) from 2010 to 2040. The fastest rates of growth are projected as 4.7 percent per year for the emerging, non-OECD regions. The strong

growth in non-OECD GDP involves the fast-paced growth in future energy consumption projected for these nations. In the OECD regions, more mature economies and slow or declining population growth trends cause a much slower growth rate of GDP as 2.1 percent per year over the projection.

High sustained oil prices determine consumer behavior on demand for liquid fuels, encouraging the use of less energy or alternative forms of energy, but also encouraging more efficient use of energy. According to U.S. Energy Information Administration (2013), energy efficiency improvements are anticipated in every end-use sector, with global liquids intensity declining (improving) by 2.6 percent per year from 2010 to 2040. On the other hand, some of the greatest potential for altering the growth path of energy use is in the transportation sector.

World net electricity generation increases by 93 percent from 20.2 trillion kilowatt-hours in 2010 to 39.0 trillion kilowatt-hours in 2040 as observed in Figure 1.3 (U.S. Energy Information Administration, 2013). The growth of electricity demand in the OECD countries is slower than in the non-OECD countries. Because electricity markets are well established and consumption patterns are mature in the OECD countries. On the other hand, in the non-OECD countries, many people do not have access to electricity at present. Total net electricity generation in non-OECD countries extends by an average of 3.1 percent per year, led by non-OECD Asia (including China and India), where annual increases average 3.6 percent from 2010 to 2040. In contrast, total net generation in the OECD countries grows by an average of 1.1 percent per year from 2010 to 2040.

In many parts of the world, concerns about security of energy supplies and the environmental effects of greenhouse gas emissions have spurred government policies that support a projected increase in renewable energy sources. As a result, renewable energy sources are the fastest growing sources of electricity generation at 2.8 percent per year from 2010 to 2040. After renewable generation, natural gas and nuclear power are the next fastest growing sources of generation, each increasing by 2.5 percent per year. Although coal-fired generation increases by an annual average of only 1.8 percent over the projection period, it remains the largest source of world power generation through 2040 (Figure 1.3). The outlook for coal, however, could be

altered essentially by any future national policies or international agreements aimed at reducing or limiting the growth of greenhouse gas emissions.

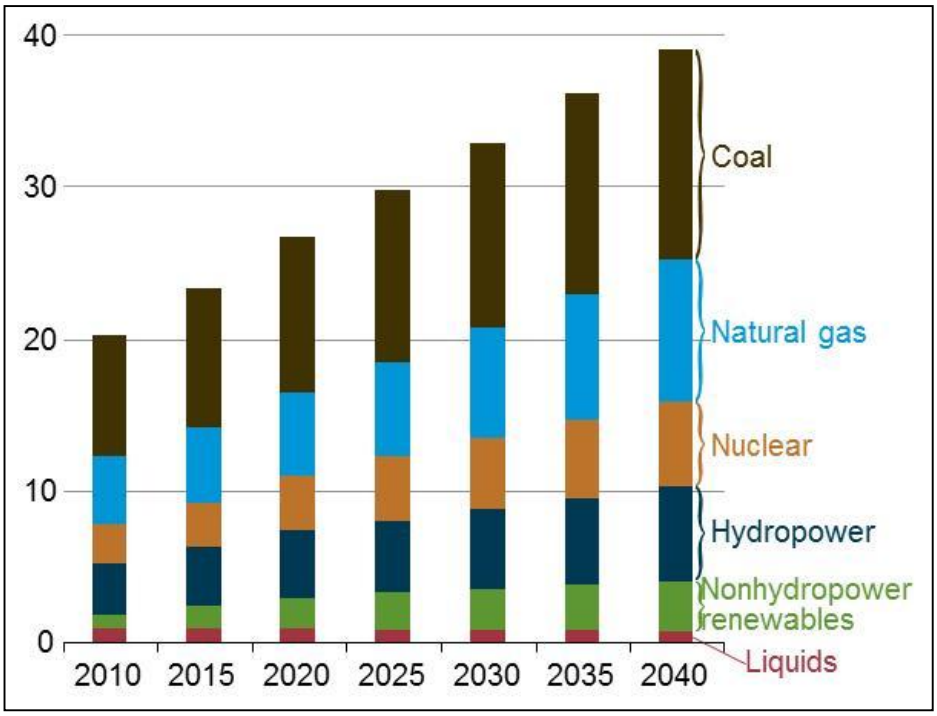

Fig. 1.3: World net electricity generation by energy source, 2010-2040 (trillion kilowatt-hours) (U.S. Energy Information Administration, 2013)

According to U.S. Energy Information Administration (2013), almost 80 percent of the projected increase in renewable electricity generation is fueled by hydropower and wind power. The contribution of wind energy, in particular, has grown rapidly over the past decade, from 18 gigawatts of net installed capacity at the end of 2000 to 183 gigawatts at the end of 2010—a trend that continues into the future. Of the 5.4 trillion kilowatt-hours of new renewable generation added over the projection period, 2.8 trillion kilowatt-hours (52%) is attributed to hydroelectric power and 1.5 trillion kilowatt-hours (28%) to wind. Most of the growth in hydroelectric generation (82%) occurs in the non-OECD countries, and more than half of the growth in wind generation (52%) occurs in the OECD countries. High construction costs can make the total cost of building and operating renewable generators higher than those for conventional plants. The intermittence of wind and

solar energy, in particular, can further hinder the economic competitiveness of those resources, as they are not necessarily available when they would be of greatest value to the system. However, improving battery storage technology and dispersing wind and solar generating facilities over wide geographic areas could help to mitigate some of the problems associated with intermittency over the projection period.

In 2010, top five countries on the list of air-conditioning imports are appeared as USA, Germany, China, France and the UK. The air-conditioning imports have increased by 20% in USA, 13.5% in Germany and 20.7% in China in 2010. Turkey has a rank of 23 on the list by importing $ 4.6 billion worth of air-conditioning systems.

Table 1.1: Imports value of air conditioning sector by country (Thousand $). HVAC-R Industry Exporters' Union, 2012.

Rank	**Country**	**2007**	**2008**	**2009**	**2010**	**Percentage Change for 2009-2010**	**Ratio for 2010**
1	USA	46,857,228	48,558,041	38,691,263	46,419,471	%20.0	%12.25
2	Germany	26,223,729	30,219,420	23,445,599	26,618,893	%13.5	%7.02
3	China	19,526,693	23,958,938	21,920,386	26,457,944	%20.7	%6.98
4	France	17,311,178	19,117,370	15,050,766	16,366,914	%8.7	%4.32
5	England	15,821,852	15,992,769	11,901,119	13,507,550	%13.5	%3.56
6	Canada	13,292,026	13,972,077	11,507,242	13,097,441	%13.8	%3.46
7	Japan	10,173,163	11,533,152	9,733,278	11,797,224	%21.2	%3.11
8	Italy	12,858,596	13,605,917	9,730,080	11,44,819	%17.6	%3.02
9	Mexico	9,952,932	10,638,534	8,453,972	10,711,359	%26.7	%2.83
10	Russia	7,327,187	10,195,695	7,435,047	10,412,392	%40.0	%2.75
11	Spain	11,367,096	10,745,565	7,847,206	8,604,125	%9.6	%2.27
12	South Korea	7,817,529	7,900,290	7,316,214	8,490,668	%16.1	%2.24
13	Belgium	8,337,844	9,687,607	7,294,823	7,729,073	%6.0	%2.04
14	Holland	7,818,444	8,601,357	6,630,459	7,220,441	%8.9	%1.91
15	Australia	5,445,098	5,899,999	6,892,756	6,346,590	%-7.9	%1.67
16	Brazil	3,534,378	4,665,018	4,221,588	6,242,628	%48.2	%1.65
17	Poland	6,000,394	7,084,066	5,435,164	5,817,505	%7.0	%1.53
18	Singapore	4,660,744	6,188,397	6,686,223	5,741,388	%1.0	%1.51
19	S. Arabia	6,659,506	3,334,824	1,632,677	5,230,075	%220.3	%1.38
20	Austria	5,524,687	6,110,690	4,906,046	5,183,005	%5.6	%1.37
23	Turkey	4,611,933	5,226,934	4,046,790	4,635,983	%14.6	%1.22
	Others	105,897,244	130,520,659	108,022,121	120,947,059	%12.0	%31.91
Total of world		**363,476,138**	**407,106,708**	**331,138,352**	**379,022,547**	**%14.5**	**%100.00**

Turkey's solar energy potential is shown in Figure 1.4 via annual total solar radiation. The region that south of the line between provinces of Izmir and Kars has a good level of solar energy potential. Mersin region seems to be one of the three regions that have the highest solar energy potential in Turkey. The other two regions are Van and Antalya.

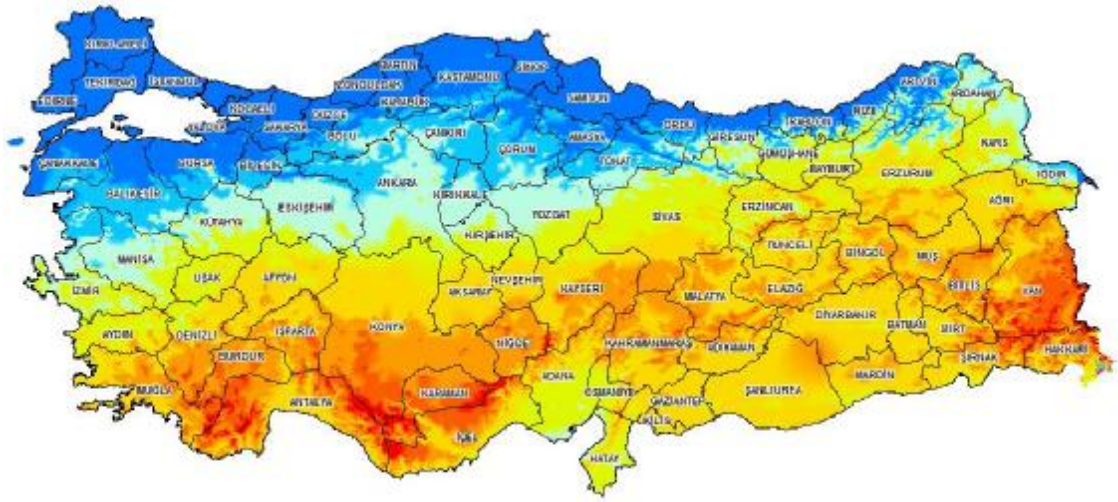

Fig. 1.4: The map of annual total solar radiation in Turkey (General Directorate of Renewable Energy, 2014)

Figure 1.5 shows the values expressed by the colors used on the map of annual total solar radiation in Turkey. Total solar radiation is over 1550 kWh/m^{2}year in the region that south of Izmir and Kars.

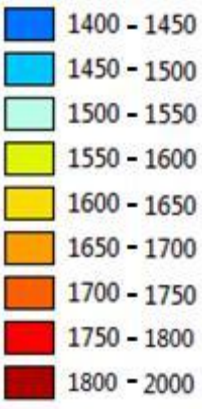

Fig. 1.5: Color scale of total solar radiation (kWh/m^{2}year) (General Directorate of Renewable Energy, 2014)

Mersin's solar energy potential is presented in Figure 1.6. Minimum value of annual total radiation is 1550 kWh/m^{2}year in Mersin. Maximum values of annual total radiation change between 1750 kWh/m^{2}year and 1800 kWh/m^{2}year. Total radiation is evaluated over 1650 kWh/m^{2}year at most of regions in Mersin.

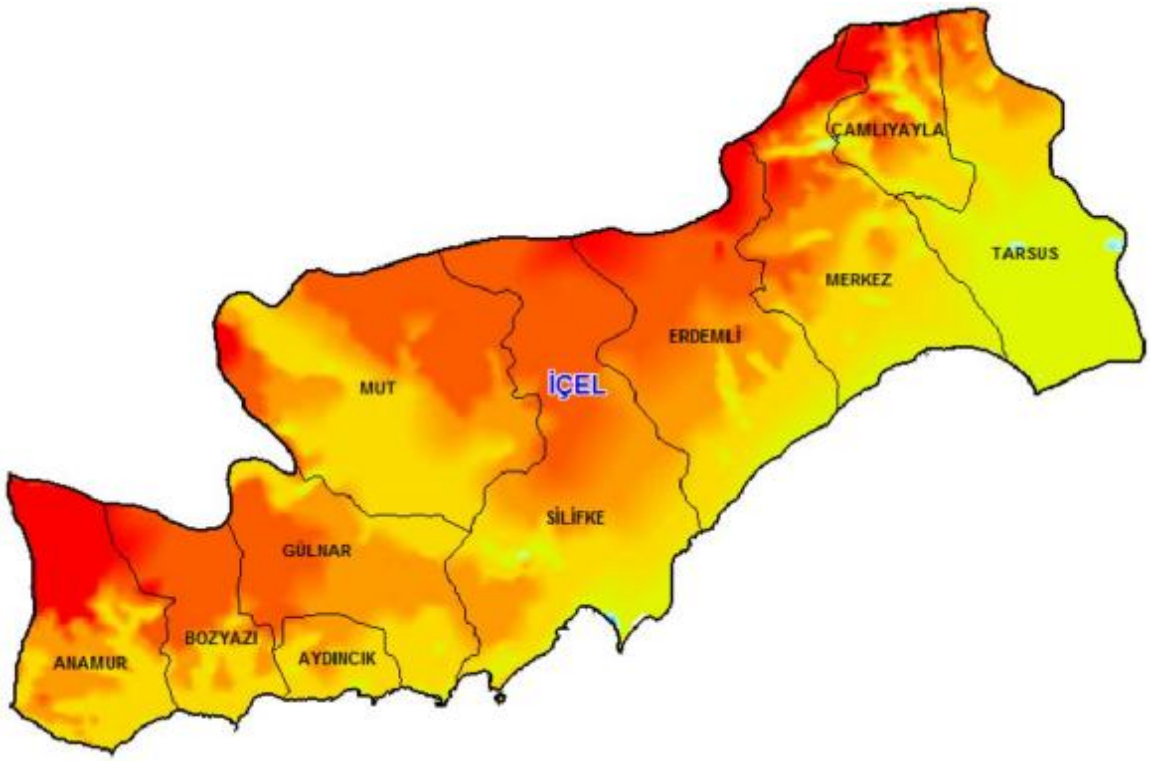

Fig. 1.6: The map of annual total solar radiation in Mersin (General Directorate of Renewable Energy, 2014)

1.3. Solar-Powered Cooling System

There are many different systems using solar energy in cooling technology. They can be presented as five main groups. (Sevinç et al., 2012)

1. The conventional vapor-compression cycle with PV
2. Thermo-mechanical refrigeration cycle with solar energy
3. Absorption refrigeration cycle with solar energy
4. Adsorption refrigeration cycle with solar energy
5. Desiccant cooling cycle with solar energy

1.3.1. The Conventional Vapor-Compression Cycle with PV

The compressor on the conventional vapor-compression cycle is operated by DC motor instead of AC motor. DC motor power is provided through photovoltaic panels. Yield of these panels change between 15 % and 17%. COP value of this system varies between 1.1 and 3.3.

1.3.2. Thermo-Mechanical Refrigeration Cycle with Solar Energy

In this cycle heat input to the system is provided by solar collectors. Especially high heat input and high temperature is required. This way, the turbine is operated by superheated steam and the compressor in the vapor compression cycle can be operated.

1.3.3. Absorption Refrigeration Cycle with Solar Energy

The absorption cooling system invented in 1860 by Ferdinand Carre and patented by him in the United State of America. Then, in 1887, absorption cooling machines were produced by the British Pontifex and Wood companies and developments have also been in this area. Especially after the 1920s, the USA, Germany, Italy, the United Kingdom, Belgium, the Netherlands, Russia and some other countries have studied the design and technology of absorption machines. After the 1950s mechanical vapor compression systems fell from grace due to cheaper electricity and construction of compressors with different capacities. (Sevinç et al., 2012)

Absorption refrigeration is one of the most appropriate methods on cooling with solar energy. The amount of energy required by the system is very low. So it may be disregarded. Working liquids are used in absorption refrigeration. These are absorbent and refrigerant pairs. The dimensions of absorption refrigeration systems are smaller than adsorption refrigeration systems because of high heat transfer

coefficient of absorbent liquid. COP values of absorption refrigeration systems range between 0.3 and 1.2.

The most important factor is performance of solar collectors to be used in the design of absorption cooling machine. If the fluid temperature reaches 150 °C, double effect absorption refrigeration machines can be used with a high COP value, in the case of the fluid temperature at 90 °C single-acting systems can be used with a lower COP value. Sevinç et al. (2012) reported in the same study, the main difference between absorption refrigeration and conventional mechanical vapor compression system is the use of absorbent refrigerant pair instead of compressor. In this way the system does not need a high electric input for the compressor.

1.3.4. Adsorption Refrigeration Cycle with Solar Energy

As reported by Sevinç et al. (2012), the refrigerant gas and adsorbent solid are used in adsorption refrigeration system. The physical and chemical reactions between these two substances operate the cycle. Refrigerant material clings to surface of absorbent material through the Van Der Waals bonds. There is no moving part in the system, so the system has a long life with this advantage. More than one adsorbent supports use for the continuity of the system and to achieve the highest COP values. Transitions between the sorption and adsorption are reason of using more than one adsorbent support. The process is intermittent with single support. The most commonly used adsorbents are activated carbon, silica gel and zeolite. The most commonly used adsorbates are water, methanol and ammonia. The primary energy input requirement of this cycle is much higher than the conventional vapor-compression cycle with PV and absorption cycle with solar energy.

1.3.5. Desiccant Cooling Cycle with Solar Energy

The sorbent is used for drying air in the desiccant cycle. The most commonly used sorbents are activated aluminum, silica gel, zeolites, LiCl and LiBr. Desiccant cooling systems ensure ventilation, humidity and temperature control. This cycle is

more effective on humidity control than the other systems. Desiccant cooling cycle with solar energy is best process especially for high ventilation or dehumidification requirement.

2. PREVIOUS STUDIES

Solar powered lithium bromide and water absorption of air-conditioning systems are used in many places around the world (Ali, 2008). As reported by Bermejo, 80 large-scale solar cooling systems were established in the worldwide in 2007, including 70 of these in Europe. (Sparber et al., 2007; Henning, 2007: Bermejo et al., 2010) The Japan Refrigeration and Air Conditioning Industry Association reported that 94.5 million units were sold in 2011. Mugnier et al. reported in the same study that the establishments of 750 solar cooling systems were completed in 2011 and developments occurred in the last seven years are indicated in Figure 2.1.

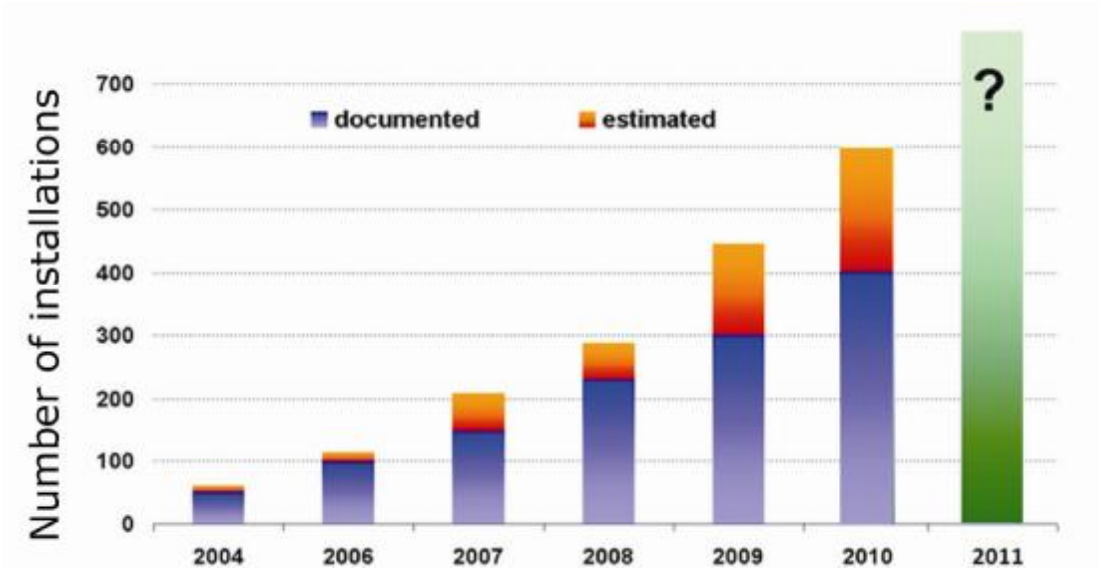

Fig. 2.1: Market development of small and large-scale solar cooling systems worldwide (Mugnier et al, 2012)

Some projects are published and reported in order to guide solar cooling systems to be installed in the future.

In the study of Eissa (1997), hydrocarbon mixture was used as a working fluid for solar absorption cooling systems. The study showed that the most appropriate fluid composed of 50% n-butane mole and 50% h-heptane mole. The working fluid operates between 55 °C and 65 °C generator temperatures and a maximum working pressure of 2.758 bars. The highest COP is 0.557 at T_G = 60 °C with cooling temperatures between 8 °C and 12 °C. Reduction of the condensing /

absorbing temperature decreases the minimum and optimum generating temperature and circulation ratio. This reduction triggers the decrease in the required solar energy for heating the generator and thus the pumping power decreases. The study reveals that reduction of the evaporator temperature has the same effect on the condensing / absorbing temperature.

Wijeysundera (1999) conducted research on the ideal three-heat-reservoir cycles with constant internal irreversibilities and external heat transfer irreversibilities in order to find the performance limits of the solar operated absorption cooling systems. COP and the cooling capacity for ideal cycle values are examined by a detailed simulation of the absorption machine. Three-heat-reservoir model with external irreversibilities and constant internal irreversibilities are used to evaluate system performance. Wijeysundera (1999) indicates that the system can be improved by adjusting the magnitude of the internal irreversibilities.

Wijeysundera (2000) studied the approximate model for the variation of the entropy transfer with storage tank temperature. COP and cooling capacity values were calculated in similar ways to the real cooling system values by adding internal entropy production to the model.

An open-cycle absorption solar cooling system in Kaohsiung, Taiwan was reviewed in the study of Yang et al. (2001). The statistical meteorological data for the summer season at Kaohsiung, Taiwan was used at a computer simulation program. The program is based on the previously obtained experimental correlations for the collector / regenerator performance. Natural convection in single-glazed collector / regenerator system was compared with the forced convection in double-glazed collector / regenerator system by the program used in this study. The C / R area, the C / R solution flow rate, the storage solution, the chilled water temperature and the daily cooling demand effect on the system performance were investigated. Results revealed that the double glazed forced convection C / R has a better performance.

Li et al. (2001) tried to improve the performance of a solar-powered absorption air conditioning system with the absorption pair of lithium bromide and water by a single storage tank having two parts. Upper part works in the morning

hours when the radiation is less intense. Both sections of the tank (upper and lower parts) are connected to the collector in the afternoon. A partitioned water tank increases the cooling period than the normal stratified water tank in order to increase cooling efficiency to a higher level.

Design and cost analysis of a domestic-size LiBr–water absorption solar cooling system with an 11 kW cooling capacity was investigated by Florides et al. (2002). The system is modeled with a simulation program. Using 15 m^2 compound parabolic collector tilted at 30° from the horizontal plane and having 600 liters hot water storage tank is most suitable for the system efficiency. Economic analysis indicates that the designed system is more appropriate than conventional cooling systems.

Grossman (2002) emphasized that solar energy equipment has a larger share in the total cost and provides higher COP; in addition, higher temperature is more expensive than lower temperature option. This study reveals the large cost difference between single and double-effect systems and the cost of the high temperature collectors prevented the use of triple-effect systems.

A solar-powered, single stage, absorption cooling system, using a water-lithium bromide solution in Antalya, Turkey was studied by Atmaca et al. (2003). The effects of hot water inlet temperatures on the COP and the surface area of the absorption cooling components were investigated using solar energy parameters.

The minimum hot water inlet temperatures were determined and the impact of COP and cooling capacity was examined. In the continuation of the study, the effects of the collector type and storage tank mass were examined.

Increasing hot water inlet temperature decreases the absorber and solution heat exchanger surface area.

The COP of system is high; on the other hand, the surface area of system components is low at high reference temperature. But, the system operates better with solar energy at lower reference temperature than the high reference temperatures.

Increasing mass of the storage tank reduces the need for an additional heat source. On the other hand, during the operation, reducing the temperature of storage

tank mass should be noticed as it does not decrease this temperature excessively. Efficient collector should be used for system efficiency despite the high prices.

Sozen et al. (2004) investigated the availability of using the ejector-absorption cooling system operated with aqua-ammonia for Turkey. Seventeen cities in different regions of Turkey were chosen to determine whether the required solar energy for the system was enough or not. The optimum values for the maximum COP values were calculated by using meteorological data obtained until 2000. Minimal additional thermal energy was calculated considering the system operates for all year. As a result of the research, the solar energy promises a great potential for cooling purposes in Turkey.

In the study of Assilzadeh et al. (2005), a solar cooling system with absorption unit for Malaysia was examined. According to the results obtained with Meteorological data, 0.8 m^3 hot water storage tank must be used to ensure continuity of system operation. A 35 m^2 evacuated tube solar collector must be used to provide 3.5 kW cooling.

The two identical systems working in the same conditions were constructed to determine the effect of cross flow of air stream with flowing film of desiccant on the surface of a solar collector/regenerator (Kabeel, 2005). One of the systems has been developed with air blower. The forced air stream flows across the absorber. So it removes the moisture from the liquid solution. The other system is considered as a control unit. Comparison of two systems showed the efficiency of the forced cross-flow system and mass transfer coefficient of designed unit was higher than the control unit.

An aqua-ammonia vapor absorption system, and an activated carbon–ammonia adsorption system with 1 m^2 collector area in Tangier, north Morocco was investigated by Ahachad et al. (2005) in December 2005. The effects of generator temperature, condenser temperature and evaporator temperature on the system were examined. The study reported that the adsorption system has a better efficiency than the absorption system.

Burns et al. (2007) examined the solar cooling systems for small commercial and institutional buildings in the Southwestern, United States. The examination

revealed that solar thermal absorption cooling systems are more appropriate options than air conditioning systems operating with electricity or fossil fuel.

The results of this study are;

- In accordance with the Energy Policy Act of 2005, 30% tax credit is applied for the solar thermal cooling systems.
- Cooling system for a five-storey building pay for itself in 8 years.
- The operating costs for smaller buildings are more suitable than conventional cooling systems.

The subject of the study of Brown et al. (2007) was a solar-powered ejector cooling-system in the cities of Antalya, Aydin, Konya and Urfa. The hourly average temperature and radiation values were used to analyze cooling system operated with an evacuated tube solar collector. The cooling season was taken as 6 months from May to October and a period between 8:00 a.m. and 05:00 p.m. were analyzed. The cooling capacity is almost same in all provinces in August, requiring evacuated-tube collector area per ton cooling is 21 m^2.

Gommed et al. (2007) tried to optimize the design by determining the performance and solving the problems with producing a prototype of the designed model. The system comprises a dehumidifier and a regenerator at the Energy Engineering Center at the Technion, in the Mediterranean city of Haifa. Also, system cleans the air in a group of offices on the top floor of the building.

Ali et al. (2008) examined the cooling system that has been working since August 2002 in Oberhausen, Germany. The system operating with solar powered single-effect lithium bromide-water absorption chiller provides the cooling in the area of 270 m^2. System operates with 108 m^2 collector area, 6.8 m^3 hot water storage tank, 1.5 m^3 cold water tank and 134kW cooling tower. The COP values vary from 0.37 to 0.81. Solar power system has contributed 8124 kWh energy to the air-conditioning system between August 2002 and November 2007.

Mazloumi et al. (2008) worked on a single effect lithium bromide-water absorption solar cooling system with a horizontal N-S parabolic trough collector in

Ahwaz, Iran. The results revealed that when the collector mass flow rate has a very small influence on the required collector area, it has a significant impact on the optimum capacity of the storage tank. The adoption of the system runs with the stored thermal energy after sundown, the minimum required collector area was found to be 57.6 m^2.

Single-effect absorption cooling system is designed and constructed at the School of Renewable Energy Technology, Phitsanulok, Thailand (Pongtornkulpanich et al, 2008). The system was established in 2005 and started to provide cooling of the test building. Data were collected during 2006 and the system using solar energy instead of conventional energy sources was examined. Evacuated tube solar collector of 72 m^2 used in the system ensured 81% of the required energy. The remaining 19% of energy requirement was provided by a LPG-fired backup heating unit.

Zambrano et al. (2008) reported the commercialization of solar cooling systems and the model operated since 2001 with solar flat collectors which feed a single-effect absorption chiller of 35 kW nominal cooling capacity. This study provides a model development and model testing with the obtained data from the actual plant. The design of an actual solar cooling system was facilitated through the simulation model.

Lecuona et al. (2009) studied the solar cooling system with single-effect lithium bromide-water absorption chillers. The study focused on small-capacity cooling systems which are suitable for domestic use or small buildings.

Eicker et al. (2009) studied the design of solar thermal absorption chillers. Their model was based on experimental data of solar cooling systems. Required vacuum tube collectors area varied between 1.7 m^2 and 3.6 m^2 as a result of the calculations. In this way, 80% of cooling was ensured. Cost analysis showed that costs were remarkably low in Southern Europe that requires high cooling.

Negation of solar air-conditioning systems without cooling or heating was shown in the study of Mateus et al. (2009). Therefore, the use of solar absorption cooling and heating systems for buildings was examined. Heating or cooling application during the year for different types of buildings such as residential, office and hotel were analyzed by a computer program. Three provinces of Europe with

different climates were selected for investigation; Berlin (Germany), Lisbon (Portugal), and Rome (Italy). Investment, operation and maintenance costs of solar cooling system were lower than conventional cooling systems.

More than 10 solar cooling demonstration projects were carried out before the establishment of the first solar cooling system in Shenzhen, China in 1987 (Zhai et al., 2009). In the study of Zhai et al. (2009), five absorption and adsorption cooling systems were examined. According to the results of analysis, solar absorption cooling systems is more suitable for the use in large buildings. Solar adsorption cooling systems gave better results in relatively small buildings. Zhai et al. proposed the use in public buildings where radiation was high.

Onan et al. (2010) researched cooling villas in Mardin, Turkey between the 15th of May and 15th of September. Cooling capacity is determined to be 106 kW as a result of the calculations.

Marc et al. (2010) investigated a solar cooling absorption system in Reunion Island, located in the southern hemisphere near the Capricorn Tropic. System was constructed and the design was controlled with the obtained experimental data. The study analyzed cooling classrooms 6 °C and 8 °C cooler than the ambient temperature without the need for any additional system. When the atmospheric temperature was very high, the cooling system could not ensure all cooling requirements. Therefore, thermal comfort was provided by ceiling fans.

The study of Tsoutsos et al. (2010) presented the performance and economic assessment of a solar heating and cooling system of a hospital in Crete, Greece. In calculations, average hourly data of 30 years obtained by Hellenic National Meteorological Service were used. The results derived by calculations allowed determining the optimum size of LiBr-H_2O system

Agyenim et al. (2010) studied the prototype of LiBr/H_2O absorption solar cooling system in Cardiff University, UK. The system was tested in summer and autumn of 2007. COP value was calculated as 0.58 with 12 m^2 vacuum tube collector area, 800 W/m^2 irradiance and 24 °C ambient temperature

The cooling system constructed in the Engineering School of Seville, Spain was tested in 2008-2009 (Bermejo et al., 2010). System operated with a double-effect

LiBr + water absorption chiller of 174 kW nominal cooling capacity. Thermal energy requirement of the system was provided by a 352 m^2 solar field of a linear concentrating Fresnel collector and a heater powered by natural gas. The main purpose of this study was to lead a desirable design of cooling systems for future. The study concentrated on the solar collector size and dirtiness, climatology, piping heat losses, operation control and coupling between solar collector and chiller.

Qu et al. (2010) studied the design, modeling, installation and evaluation of solar cooling and heating system at Carnegie Mellon University in Pittsburgh, USA. The system operated with the area of 52 m^2 of linear parabolic solar collectors using 16 kW of energy and the water–lithium bromide (LiBr) absorption chiller. Qu et al. (2010) indicated that the investigated system was the smallest for high temperature of the solar cooling system in the world. Solar thermal ensured 39% of cooling energy and 20% of heating energy when it was appropriately installed.

The study of Sanjuan et al. (2010) tried to combine a solar absorption cooling system with a bioclimatic building constructed in the Plataforma Solar de Almeria (PSA) in Spain in the recent time. The designed absorption heat pump system consisted of 4 heat pumps. There was no need for an additional storage tank because heat pumps stored energy with crystallized salts. The heat pump consisted of two separate barrels. Barrels were recharged by the sun and could be discharged in order to provide heating or cooling.

A solar powered absorption cooling installation was observed between 2007 and 2008 and was compared with the obtained data from a detailed computer simulation (Monnin et al., 2011). Analytical and experimental results showed a decisive impact of the cooling water temperature and the generator driving temperature on the COP. The study showed that COP values could be increased by 42%.

Desiccant cooling systems supported by air heater collectors examined in 2010 (Sevinç et al., 2012). Desiccant systems were investigated in three different climates. These are single-stage desiccant system. They have established a factory in Althengstett / Germany, a library in Mataro / Spain and a laboratory in China.

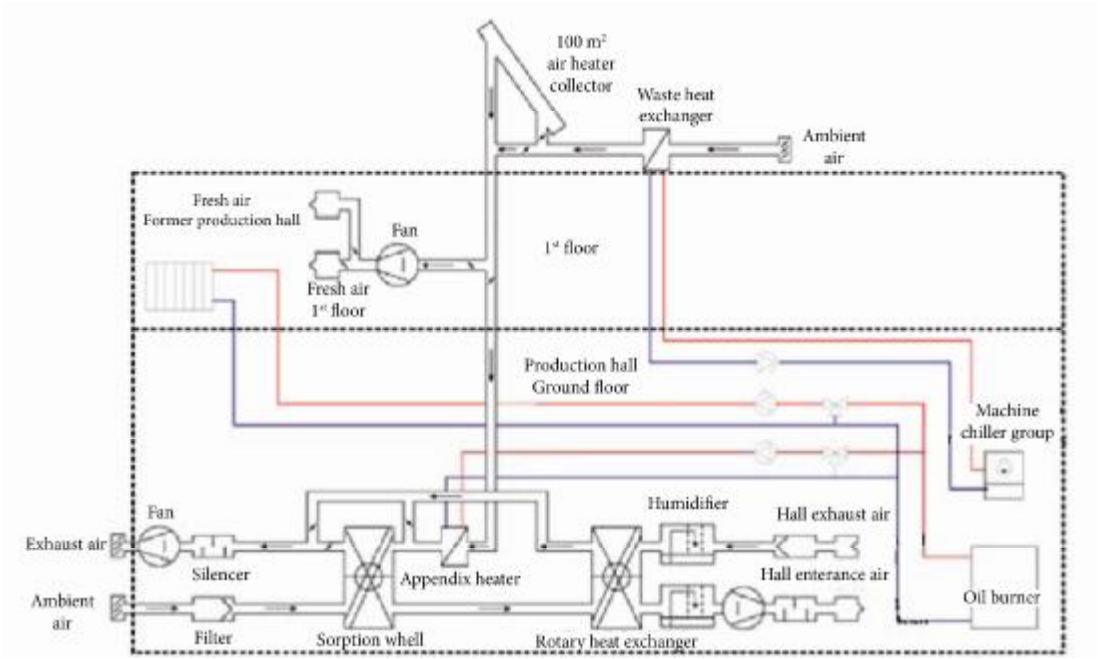

Fig. 2.2: Desiccant cooling cycle with solar energy in factory of plastic in Althengstett / Germany. (Sevinç et al., 2012)

The schematic representation of the system in Althengstett is observed in Figure 2.2. Cooling space that 800 m^2 is cooled by air heater collector that have 100 m^2 areas. System can be cooled at 17 °C that is a minimum temperature. Air flow processed to pre-heated as 45 kW by using LiCl was used in sorption cycle.

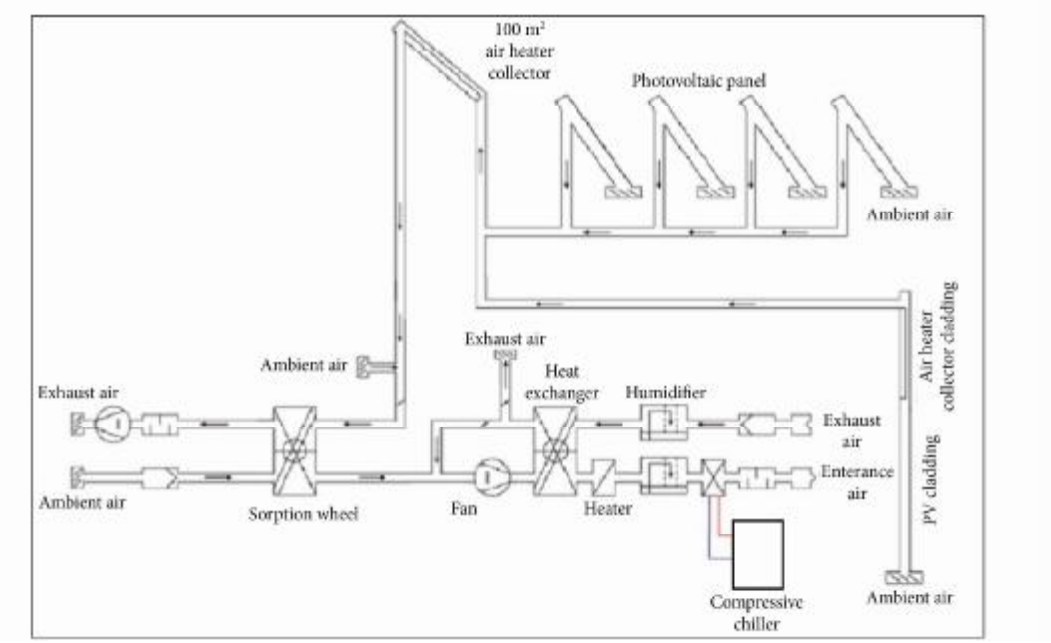

Fig. 2.3: The public library in Mataro / Spain that cooled by desiccant cooling system. (Sevinç et al., 2012)

The public library in Mataro / Spain that cooled by desiccant cooling system is observed in Figure 2.3. The system cools 3500 m^2 area. The system also includes PV panels that have 55kW power. There is a ventilation for cooling these panels. On the other hand, the waste heat is also used in the process. The air heater collector area that used in the system is 155 m^2. Only 9% part of cooling operated with maximum flow rate (12000 m^3/h). And 24% part of cooling operated with flow rate between 6000 m^3/h and 12000 m^3/h. 27% part of cooling operated with 6000 m^3/h flow rate. In this way, there is a large amount of energy saving in the consumption of the electricity.

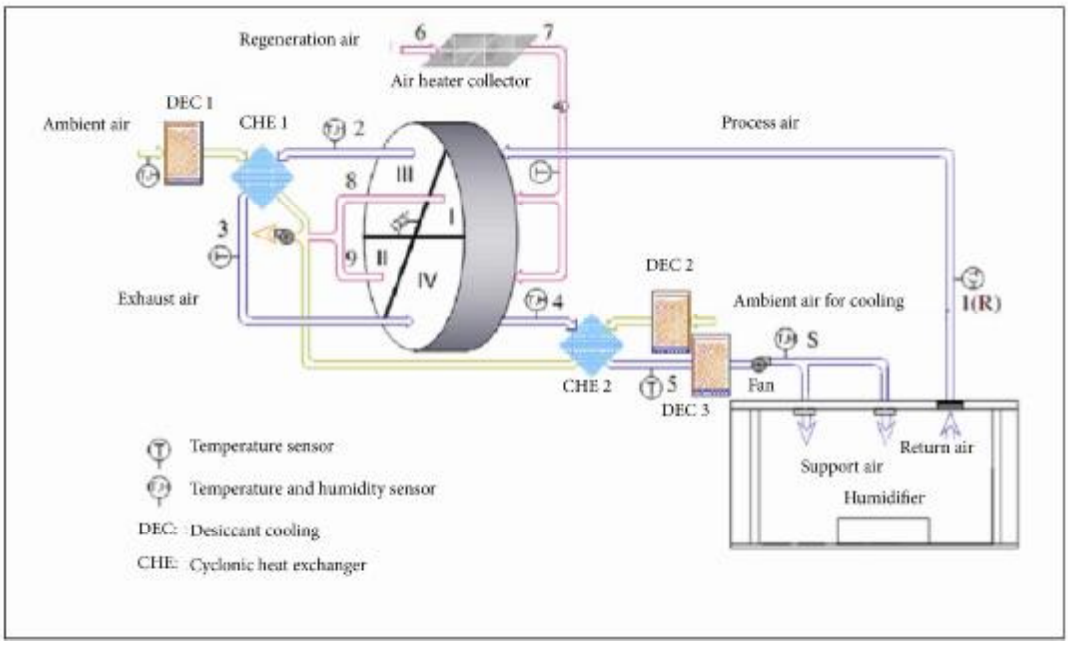

Fig. 2.4: Solar desiccant system installed in a laboratory in Shanghai/China. (Sevinç et al., 2012)

Figure 2.4 shows two stages desiccant system installed in Shanghai/China. This system is smaller than the other two systems. It operates for cooling a laboratory that had a 72 m^3 volume. Maximum cooling load of the system is about 4.5 kW. Three vacuum tube air collectors are used for regeneration. Performance values of these three different systems are observed in table 2.1. The COP values decreases due to low yield of heat recovery.

The average value of COP in Mataro was calculated as 0.6 for regeneration temperature at 75 °C. Average COP for the system in Shanghai was calculated as 0.95. And the average COP value of desiccant cooling system in Althengstett was calculated as 0.5.

Table 2.1: Performance values of desiccant cooling system components that located in three different regions (Sevinç et al., 2012)

	Mataro	**Althengstett**	**Shanghai**
Efficiency of dehumidification	80	80	88
Efficiency of humidification	86	85	82
Efficiency of heat recovery	68	62	70/67

3. METHODOLOGY

3.1. Modeling Solar Powered Absorption Refrigeration System

3.1.1. The Working Principle

Solar absorption cooling systems consist of three main parts: a solar collector, a storage tank and an absorption chiller cooling. In addition, an absorption chiller consists of four heat exchangers: generator, condenser, evaporator and absorber (Mazloumi, 2008).

The rich ammonia solution leaves the absorber. The solution heated by passing through the heat exchanger by a pump comes to the generator. The refrigerant (ammonia) vapor is separated from the solution by granting the heat from the solar collector in generator. Ammonia vapor leaves the generator and enters to the condenser. The weak solution remaining in the generator passes the heat exchanger and heats the rich solution then returns to the absorber.

The ammonia vapor entering to the condenser transfers heat to environment by condensing process.

The ammonia leaving the condenser in the form of saturated liquid or compressed liquid phase is expanded in order to reach the evaporator pressure with the help of an expansion valve. Evaporating ammonia takes the necessary heat from the cooling space in the evaporator. The ammonia vapor leaving the evaporator in the phase of saturated steam or superheated steam enters to the absorber.

The weak solution releases heat by passing the heat exchanger. The pressure of poor solution is decreased to a value of absorber pressure by an expansion valve to absorb the ammonia vapor that comes from the evaporator and then heat is released in the absorber. The heat must be taken from the absorber for the efficiency of absorption process. The solution which becomes rich in terms of ammonia is delivered to the generator again by means of a pump. The rich solution from absorbers is heated by the weak solution returned from the generator in the heat exchanger to reduce heat losses. An external mechanical energy is not needed for

system operation except for a small amount of energy supplied to the pump. The system works with the heat energy given to the generator.

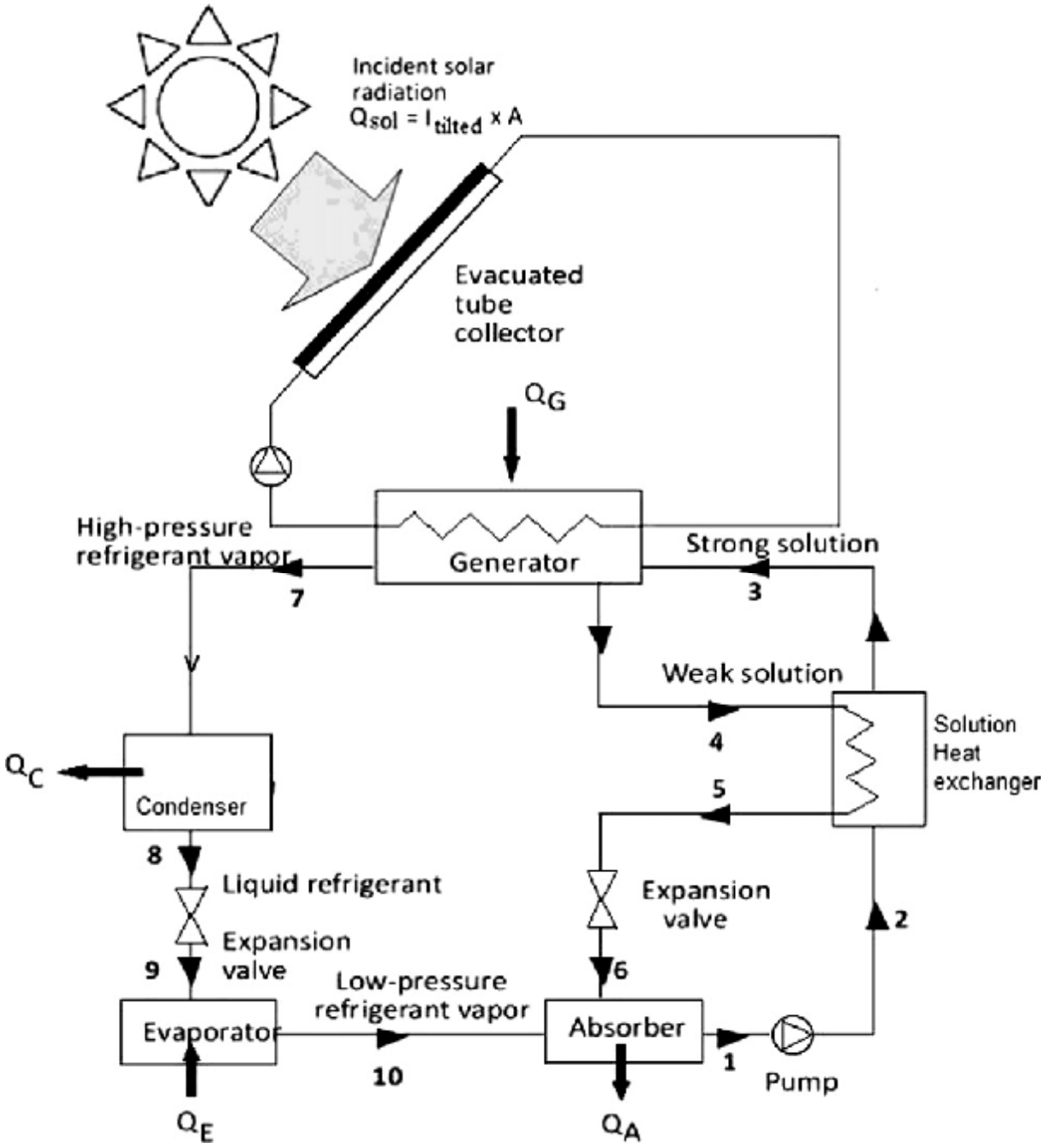

Fig. 3.1: Components of the solar absorption refrigeration system (Ozgoren et al., 2012)

3.1.2. The Solar Collector

The solar collectors have a great importance for the main energy source of system is sun. Efficiencies of solar collector directly affect the system performance for bringing on the system; the heat energy produced by falling solar radiation. The collector is carefully selected to receive maximum benefit from solar energy. There are many types of collectors used for different purposes. Flat-plate collectors are most commonly used in residences.

The cold fluid which comes from the tank enters the collector from the lower part. Fluid is heated up by radiation received from the collector when it passes through a series of the copper pipes. Heated fluid rises with natural convection or support of a pump and accumulates in the tank. Efficiency of flat-plate collectors is improved at the present time by the addition of a second reflective glass or selective surface.

3.1.3. Evacuated Tube Solar Collector

Evacuated tube solar collector has been used as a result of the development of solar collectors. It has been developed by parallel connection of several tubes according to the requirement. Tubes consist of two interwoven glass pipes which have a vacuum between them. Cold liquid enters inlet of the inner tube. While this cold liquid moves upward direction, it is heated. The heated liquid rises vertically and reaches the tank. Namely, repeating cycles keep the liquid warm in the tank. Vacuum tube collectors receive perpendicular sun rays when it is in the same direction as a flat plate collector. Because of its design, vacuum tube collectors capture almost all of the radiation reflected from the absorber plate. Their efficiency is much higher than the flat plate collectors. The disadvantage of vacuum tube collectors is their higher cost than the conventional flat-plate collectors.

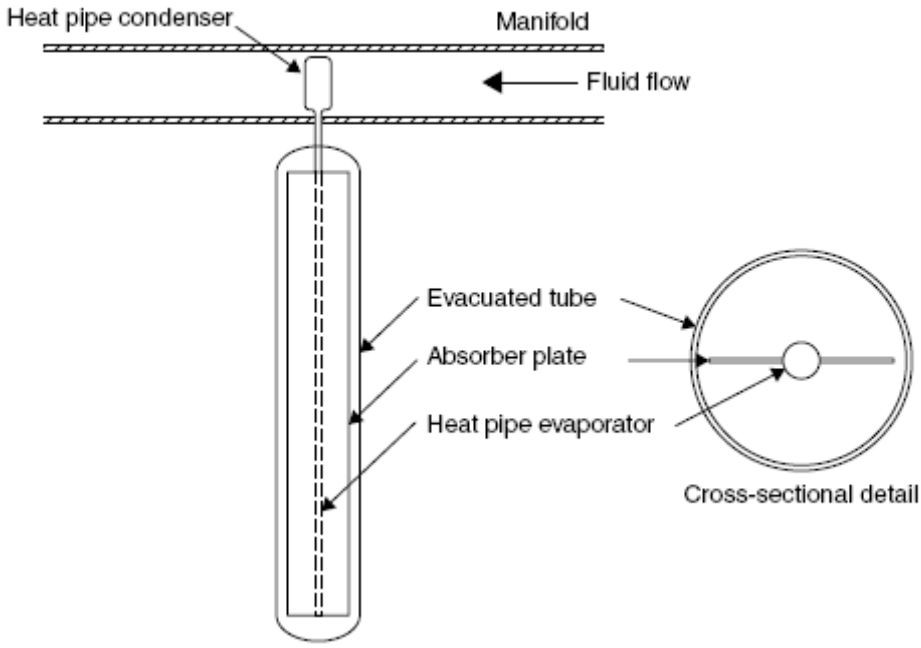

Fig. 3.2: Schematic diagram of an evacuated tube collector (Kalogirou, 2009)

3.1.4. Refrigerant-Absorbent Pairs

Lithium bromide and ammonia water solutions are most widely used as the working fluid in absorption systems (Lecuona, 2009). Florides (2002) stated that the most commonly used refrigerant-absorbent pairs are water-lithium bromide (LiBr) and ammonia-water. These couples have the best thermodynamic performance and are environmentally friendly. The ammonia-water pair requires high temperature (125-170 °C) in generator. The water-LiBr pair has a lower temperature than the temperature needed in the generator (90-120 °C). Single-effect lithium bromide-water (LiBr-H_2O) chiller is the most common solar cooling system which can be operated at a lower temperature. Double-effect LiBr-H_2O machines are observed in some systems which operate at temperature around 150 °C. LiBr-water absorption cooling systems are widely used as an air-conditioning as a result of good performances and low costs. For working with low levels of energy, they can be used with renewable energy sources as the working liquid needs a low level of temperature and they are environmentally friendly (Mazloumi, 2008).

The different advantages and disadvantages are determined in the comparison of LiBr-H_2O solution and ammonia-water solution (Yamankaradeniz, 2009).

- LiBr-H_2O can not be used below 0 °C. But, ammonia-water solution can operate at very low temperatures. Ammonia-water solution can be used at deep-cooling applications due to this feature.
- Ammonia leak is easy to be recognized because of the smell, while water leakage is not easy to be recognized.
- Ammonia is a toxic and carcinogenic substance, while the water is harmless.
- Ammonia damages the copper and copper alloy material. Therefore, steel must be used in the system, which increases the cost. However, water does not damage the copper and copper alloy material.
- Ammonia saturation pressure is high, and for this reason, excess material thickness is required in this system.
- Saturation pressure of water corresponding to the evaporator temperature is very small, so the system is at risk of containing air. There is no such problem with ammonia-water solution.
- There is a relocation risk of a small amount of water at line between generator and the condenser for ammonia-water solution. For this reason, rectifier or analyzer must be used at the output of generator.
- The systems using LiBr-H_2O solution are at risk of turning LiBr into crystal structure. Special apparatus must be used to prevent this problem.
- The value of $COP_{cooling}$ is around 0.5 for Ammonia-water solution; on the other hand, the value of $COP_{cooling}$ is around 0.7 for LiBr-H_2O solution.

3.1.5. Thermal Storage Tank

The use of a thermal storage tank is a common practice because the energy provided by solar energy doesn’t correspond to the needed solar energy for each hour. For this reason, surplus energy can be stored for this application as heating

energy when solar energy is less than required. Thus, it would be possible to utilize the system both for longer time and higher efficiency.

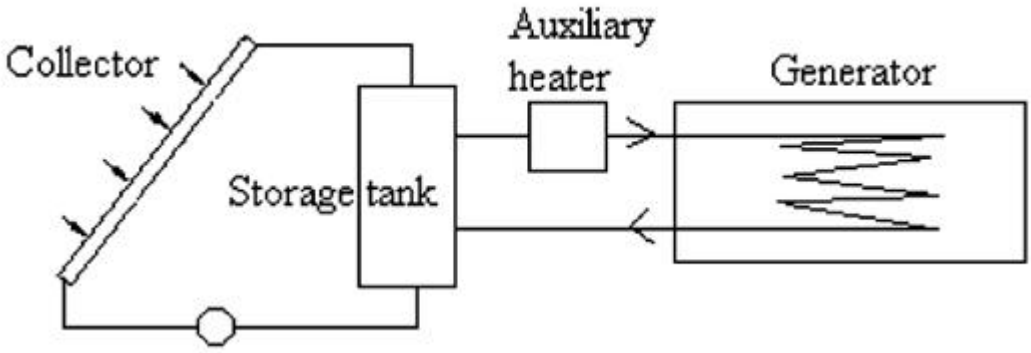

Fig. 3.3: Usage of solar energy in the system in detail (Atmaca et al, 2003)

3.1.6. Refrigerated Space

Determining the cooled space is one of the primary stages of the study. The refrigerated area is the room shown in Figure 3.4. Refrigerated area is located south and west exposure. Refrigerated area is on the fourth floor of the seven-storey building. There are two windows with 2 m × 2 m size on both exposures. Exterior wall thickness is 0.2 m and interior wall thickness is 0.1 m. refrigerated area size is 5 m × 6 m and its area is 30 m^2. Height is 3 m and refrigerated space volume is 90 m^3. Wall transmission is taken as 25 m^2. Window and skylight solar loads are taken as 8 m^2.

When cooling load for the selected space is calculated, overhead lighting is taken as 750 W and Electric Equipment is taken as 500 W. Four people are supposed to live in the cooled area and 130 W loads per person are taken. Safety factor is 15%. Heat gain through doors, floor and ceiling are taken as zero with acceptance of all floors that are refrigerated separately. It is assumed that infiltration and ventilation do not occur.

3.1.7. Cooling Season

The hourly average atmospheric temperatures are obtained to determine the cooling season. By considering human comfort, cooled space temperature is taken as 24 °C. According to temperatures at 02:00 pm, temperatures begin to increase after the 5th of February when the lowest value of temperature is seen. The temperature rises until the 5th of August and then begins to decrease. Reduction continues until the 19th of December. Between December and February, the temperature varies from 13 °C to 16 °C.

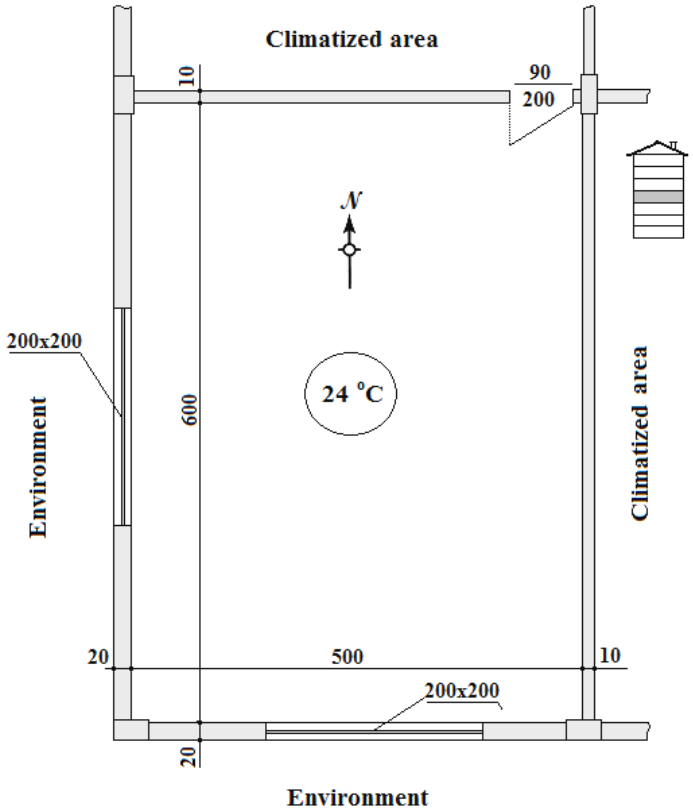

Fig. 3.4: Schematic representation of the refrigerated space

Daily values of average temperature and radiation at 02:00 pm are observed in Figure 3.5. The average temperature reaches 24.7 °C on the 4th of May. It reaches 31.9 °C on the fifth of August and then decreases until November 2 and reaches 24 °C. Cooling season is considered between May and October when temperatures are

higher than 24 °C. However, radiation decreases from 590 W on the 26th of September to 373 W on the 29th of October, so season between May and September is an appropriate choice for cooling.

The cooling season is taken as five months from May to September by considering average temperatures of Mersin.

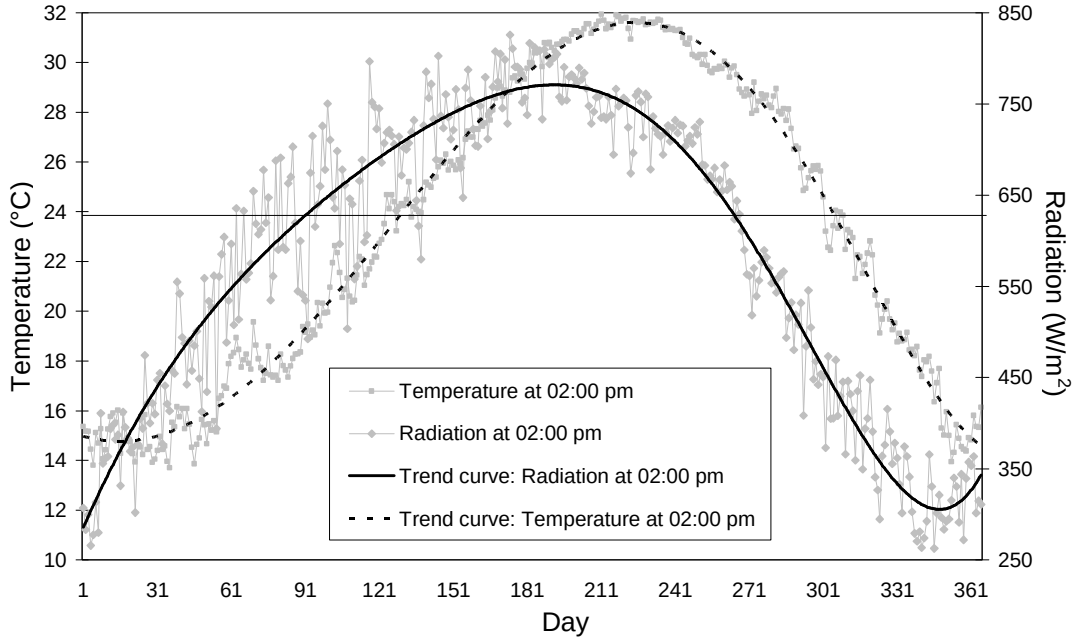

Fig. 3.5: Daily values of average temperature and radiation at 02:00 pm

Table 3.1 shows temperatures and duration of insolation values in Mersin on cooling season (Turkish State Meteorological Service). The average temperature values in August are taken highest values compared to six months. Also the highest temperature is measured in August as 39.80 °C.

Minimum average duration of insolation value is 7.5 hours in October. In summer the average duration of insolation values are shown as minimum 10 hours. The average temperature values in September are higher compared to values in June. Therefore cooling is necessary in September more than June.

The average temperature values in May and October are nearly equal together. And the highest average temperature value in October is higher than May. However average duration of insolation value in October is 7.5 hours. Thus cooling

season excludes October with taking the lower radiation and duration of insolation values into account.

Table 3.1: Temperatures and duration of insolation values in Mersin on cooling season (1954-2013) (Turkish State Meteorological Service)

MERSIN	**May**	**June**	**July**	**August**	**September**	**October**
Average temperature (°C)	21.40	25.20	27.90	28.30	25.50	21.10
The highest average temperature (°C)	24.80	28.10	30.70	31.40	30.00	26.80
The lowest average temperature (°C)	16.80	20.80	24.00	24.20	20.90	16.40
The average duration of insolation (hour)	8.50	10.10	10.10	10.00	9.20	7.50
The highest temperature (°C)	35.80	38.20	37.30	39.80	38.50	36.40

Degree Day (D/D) is a unit that shows the amount of 24 hours period for cold and warm conditions (Turkish State Meteorological Service).

Heating Degree Days (HDD) explains the intensity degree of cold condition with taking the atmospheric temperature and room temperature in a determined time into consideration. A lot of countries use different definition for calculation of degree day. Eurostat (European Commission Statistical Agency) proposes the method to calculate HDD for comparable and common use. HDD is calculated by subtract average daily temperature (T_m) from 18 °C, if T_m is equal to 15 °C or lower. If T_m is higher than 15 °C, HDD is taken as zero.

HDD is calculated for daily period. Monthly and yearly HDD are total of daily values in monthly and yearly periods.

Relatively Heating Degree Day is ratio of current degree day and average degree day at long period.

The definition of Cooling Degree Days (CDD) is the intensity of heat that calculated with atmospheric temperature for a period time. There is no formal threshold temperature, on the other hand, threshold temperature is taken as 22 °C in the construction sector. CDD is calculated by subtracting 22 °C from the average

daily temperature (T_m), if T_m is equal to 22 °C or higher. If T_m is lower than 22 °C, HDD is taken as zero.

The necessity of Total Degree Day

1. Total of Heating or Cooling Degree Day is important to know required energy for heating or cooling purposes. Heating is unnecessary when atmospheric temperature is higher than 15 °C. Heating cost is directly proportional with HDD. Heating price for 1 HDD is calculated as a yearly fuel cost divided by yearly HDD. Then this value uses in other calculations. Namely, this is practical method for calculating fuel cost.

2. HDD is also used for comparison of winter intensity according to last years.

3. HDD is required parameter for construction sector to calculate expense of insulation, heating and cooling systems.

Table 3.2 shows cooling degree days and the number of days in which the temperature is above 22 °C in May to October between 2008 and 2014. Every day in June to September, cooling is necessity in Mersin. The highest values of cooling degree days are observed in August. The necessary of cooling in October is more essential as compared to May. On the other hand lower radiation and duration of insolation values are disadvantage of solar-powered cooling in October.

Table 3.2: Cooling Degree Days and The number of days in which the temperature beyond 22 °C from May to October in Mersin (2008-2014) (Turkish State Meteorological Service)

Location	**D/D**	**Months**					
MERSIN		**May**	**June**	**July**	**August**	**September**	**October**
2014	CDD	22	110	215	232	148	29
	T>22 °C	15	29	31	31	30	17
2013	CDD	61	131	226	244	147	10
	T>22 °C	25	30	31	31	30	11
2012	CDD	15	143	238	249	186	57
	T>22 °C	13	30	31	31	30	20
2011	CDD	22	114	218	249	175	
	T>22 °C	9	30	31	31	30	
2010	CDD	36	127	215	278	205	
	T>22 °C						
2009	CDD	28	149	218	234	124	
	T>22 °C						
2008	CDD	25	140	232	253	165	
	T>22 °C						

Net radiation and temperature values are basic criterions for calculation of solar-powered cooling. Therefore, variations radiation and temperature are considerable subject to research.

Figure 3.6 shows net radiation in May 2014. Net radiation is higher on northern hemisphere in for the period from May to August. Turkey's geographical location is 36 °- 42 ° north latitude. This location is termed as Sun Belt. Turkey owns high solar energy potential and duration of insolation.

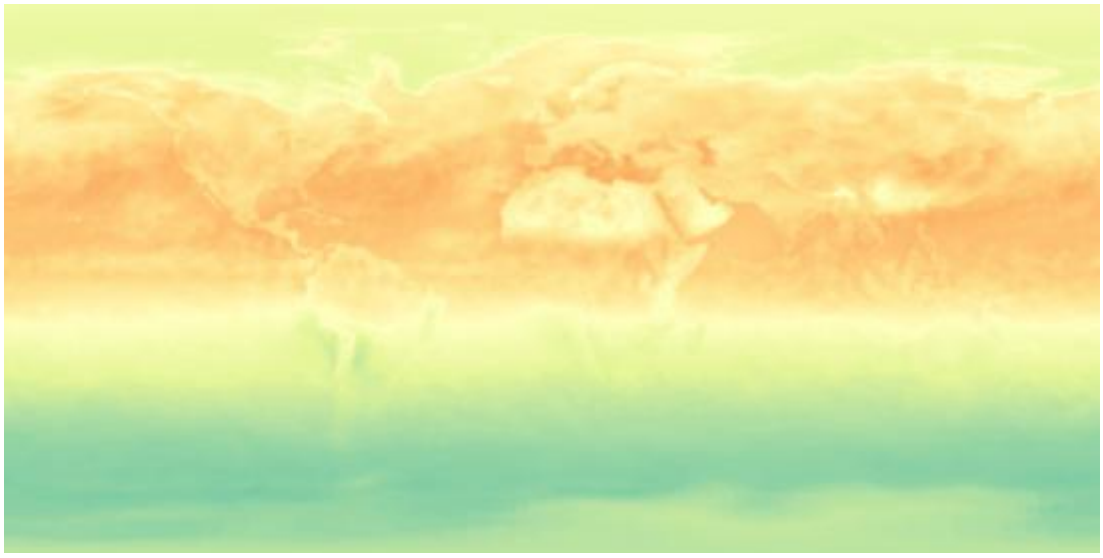

Fig. 3.6: Net radiation map of earth in May 2014 (NASA Earth Observations)

Figure 3.7 observes net radiation in June 2014. Net radiation values of Turkey are high in June. This situation provides a good opportunity to use solar-powered cooling systems in Turkey.

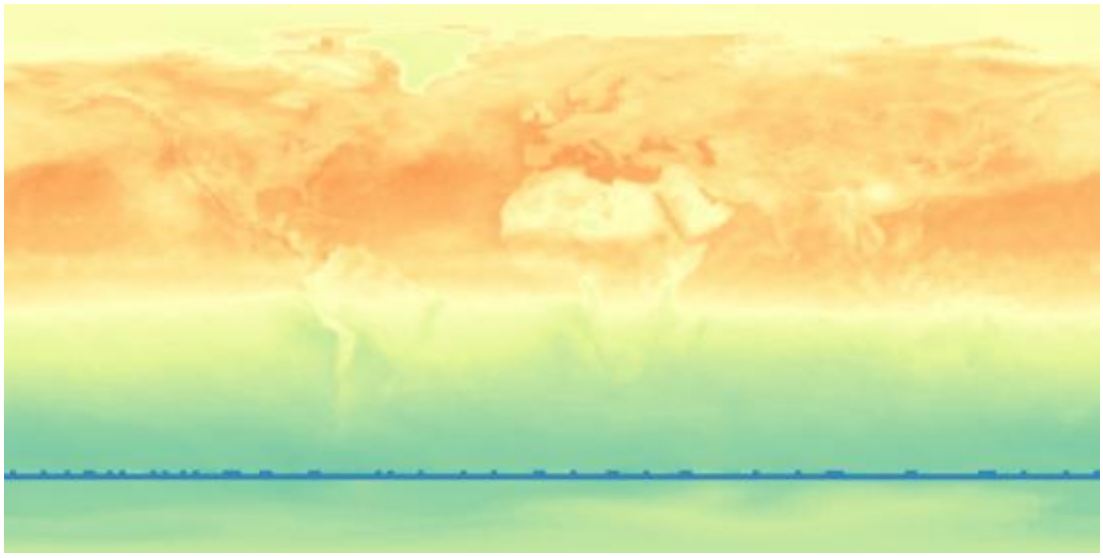

Fig. 3.7: Net radiation map of earth in June 2014 (NASA Earth Observations)

Net radiation in July 2014 is observed in Figure 3.8. Rising of net radiation values in Turkey continued in July. Thus net radiation values are suitable for solar cooling systems.

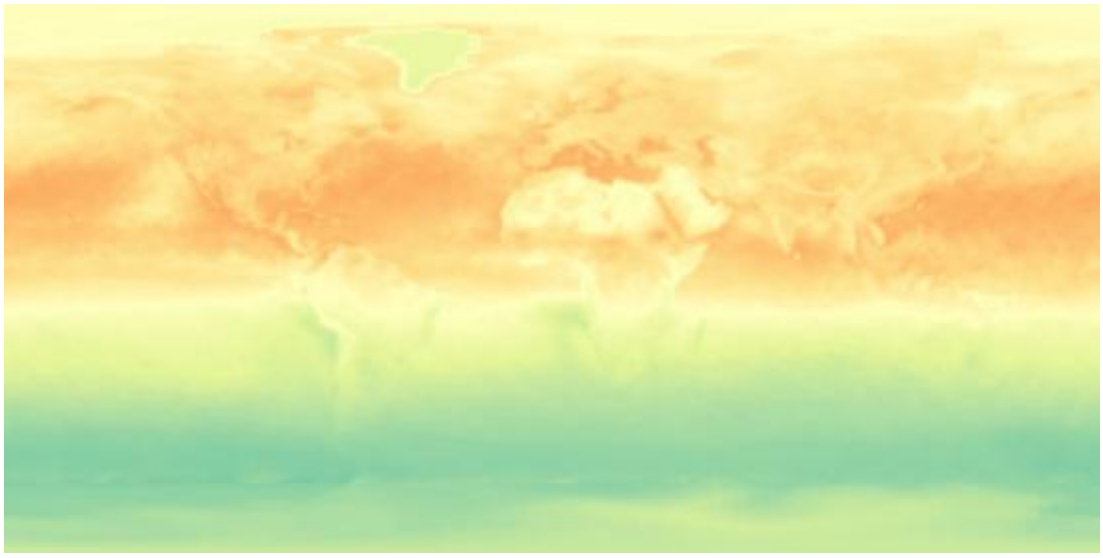

Fig. 3.8: Net radiation map of earth in July 2014 (NASA Earth Observations)

Net radiation in August 2014 is showed in Figure 3.9. The highest net radiation values of Turkey are observed in August. Temperature values are also taken the highest values in August. Necessity and facility of solar-powered cooling are shown together in August.

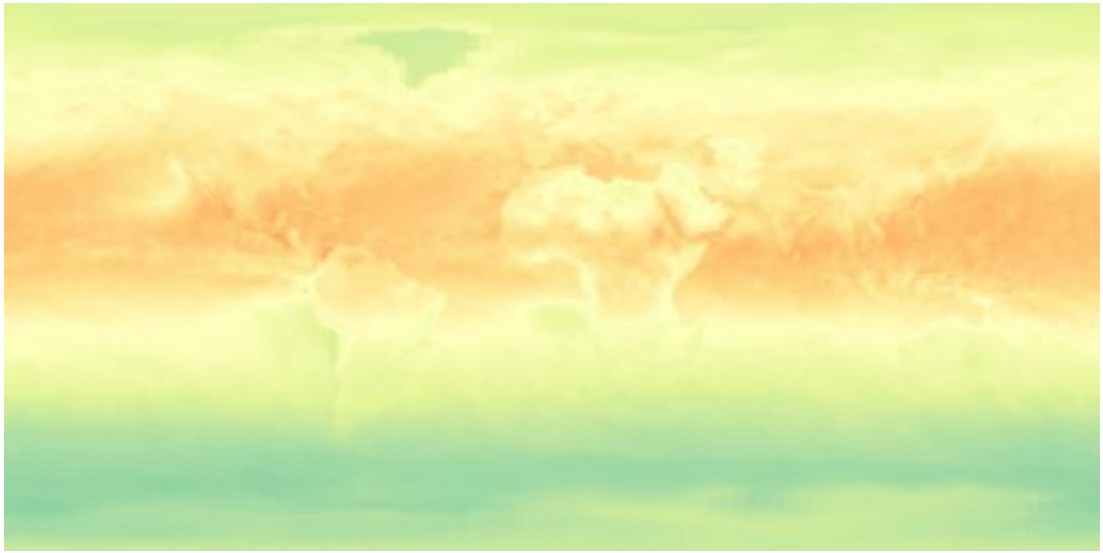

Fig. 3.9: Net radiation map of earth in August 2014 (NASA Earth Observations)

Figure 3.10 shows net radiation in September 2014. Reduction of net radiation in September is observed in net radiation map of earth in September 2014.

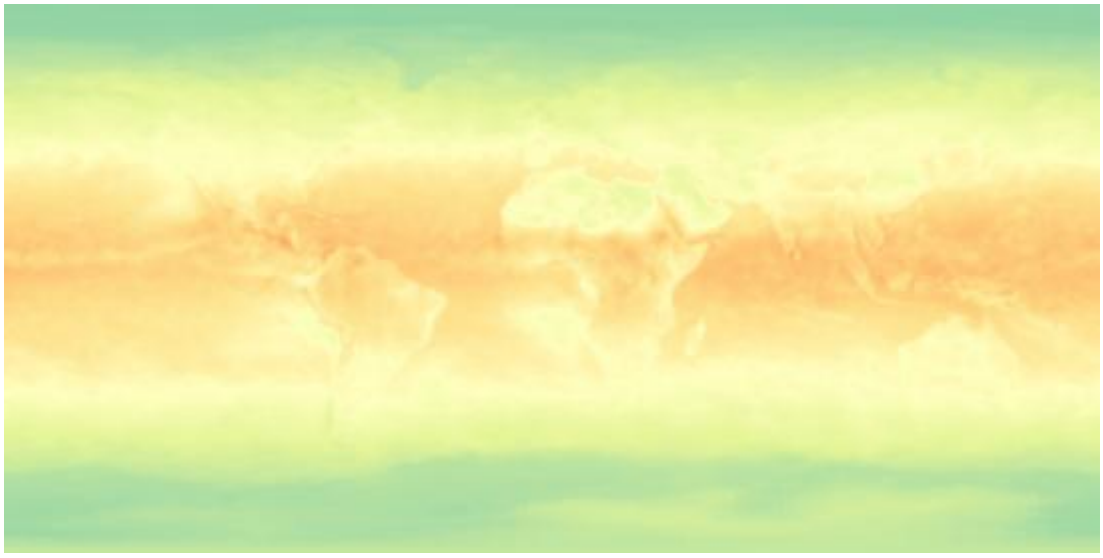

Fig. 3.10: Net radiation map of earth in September 2014 (NASA Earth Observations)

Figure 3.11 shows color scale of net radiation map of earth. The minimum net radiation value is -280 W/m^2 on the scale. The maximum net radiation value is 280 W/m^2.

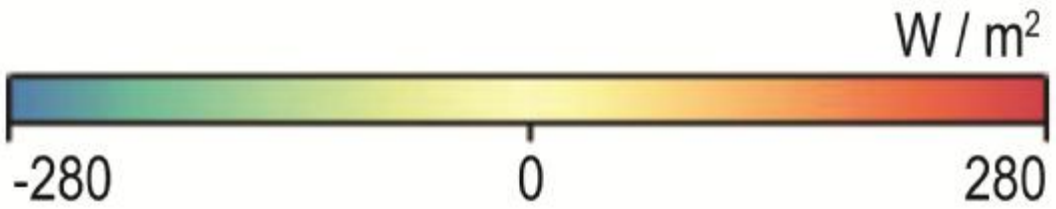

Fig. 3.11: Color scale of net radiation map of earth (W/m^2) (NASA Earth Observations)

Thermal infrared measurements used to make daytime land surface temperature maps. The Moderate Resolution Imaging Spectroradiometer (MODIS) instrument aboard NASA's Terra and Aqua satellites measured thermal infrared values. Land surface temperature is a good indicator of the energy balance at Earth's surface (NASA Earth Observations).

Figure 3.12 shows land surface temperature in May 2014. Land surface temperature in Turkey requires cooling in May. The values reached above 22 °C on most of days in May.

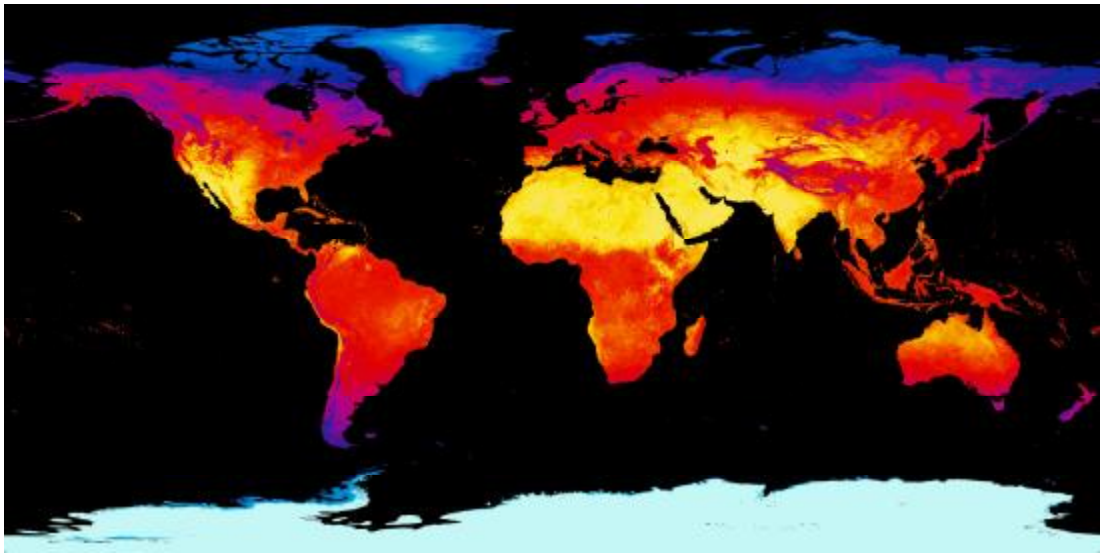

Fig. 3.12: Daytime land surface temperature map of May 2014 (NASA Earth Observations)

Figure 3.13 observes land surface temperature in June 2014. Land surface temperature values in June are shown as higher than May in Turkey.

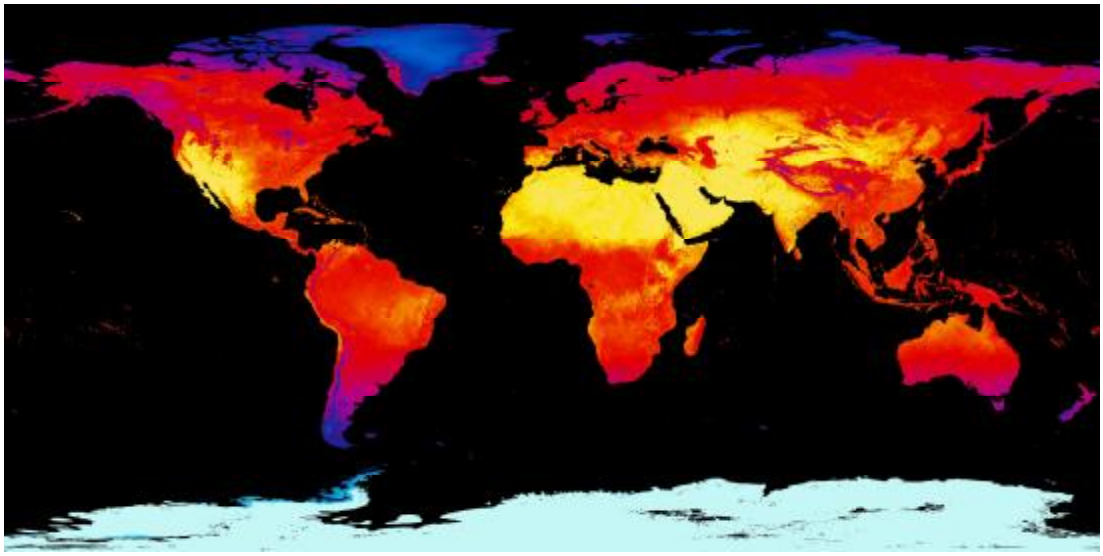

Fig. 3.13: Daytime land surface temperature map of June 2014 (NASA Earth Observations)

Land surface temperature in July 2014 is showed in Figure 3.14. Rising of temperature values in Turkey continued in July 2014. Thus land surface temperature values in July are observed as higher than June.

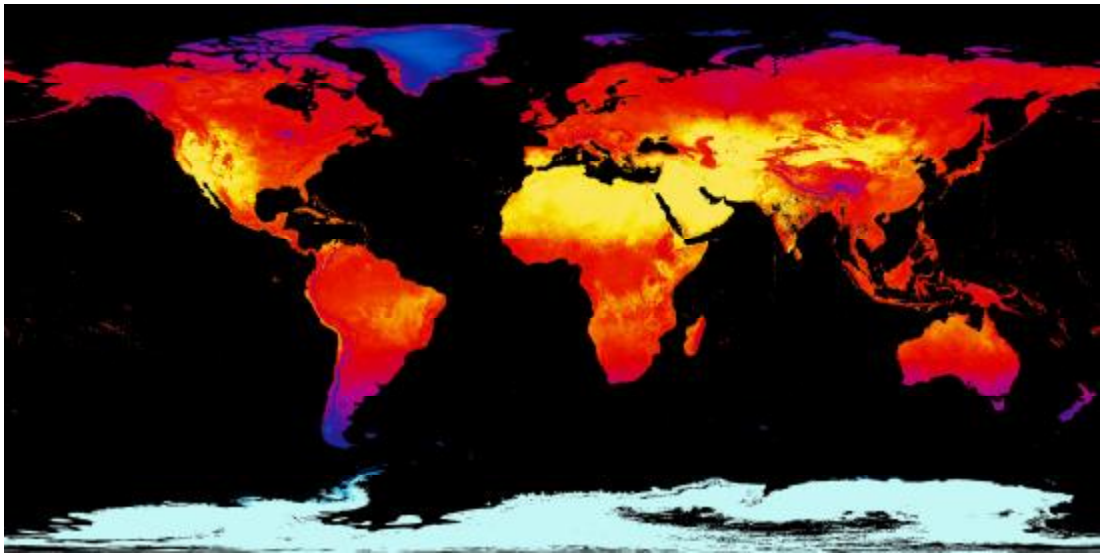

Fig. 3.14: Daytime land surface temperature map of July 2014 (NASA Earth Observations)

Land surface temperature in August 2014 is observed in Figure 3.14. Temperature values reached the highest level in August. Therefore most of region of Turkey showed with yellow in Figure 3.15.

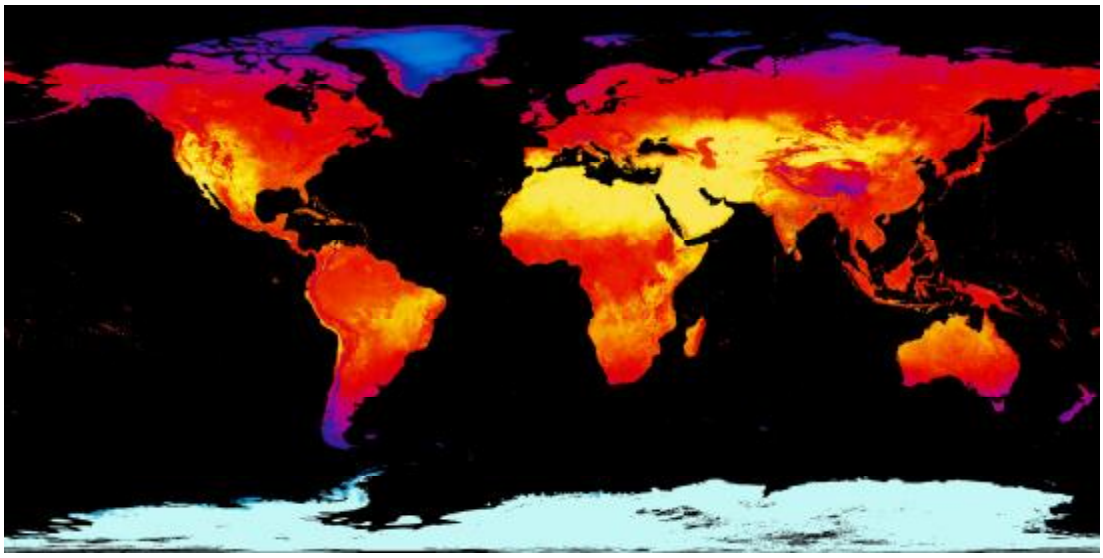

Fig. 3.15: Daytime land surface temperature map of August 2014 (NASA Earth Observations)

Figure 3.16 shows land surface temperature in September 2014. In September, there was a relative decrease in temperature in Turkey. On the other hand, land surface temperature values are observed as higher than May.

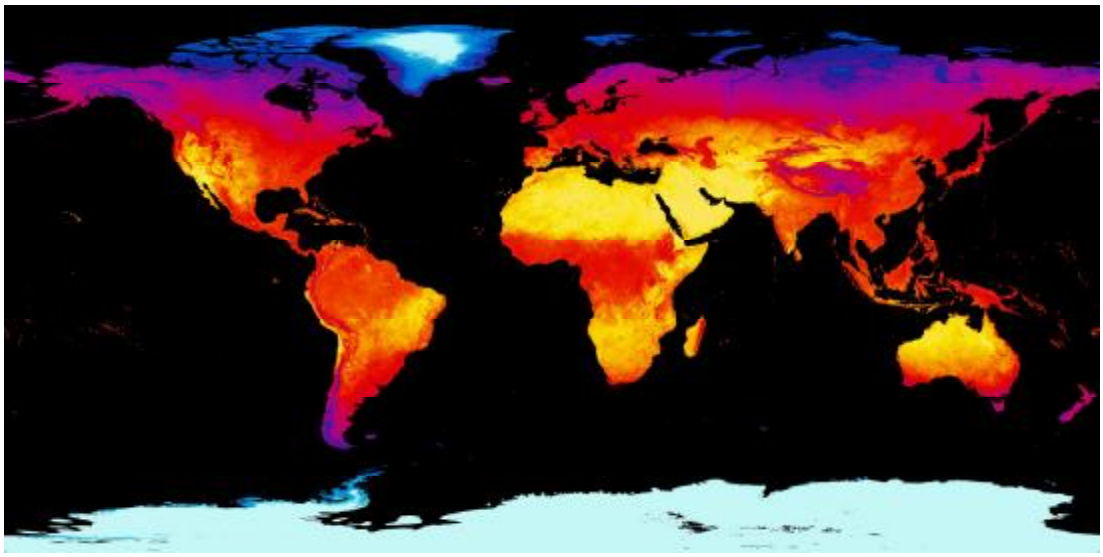

Fig. 3.16: Daytime land surface temperature map of September 2014 (NASA Earth Observations)

Figure 3.17 shows color scale of land surface temperature map of earth. The minimum net radiation value is -25 °C on the scale. The maximum net radiation value is 45 °C.

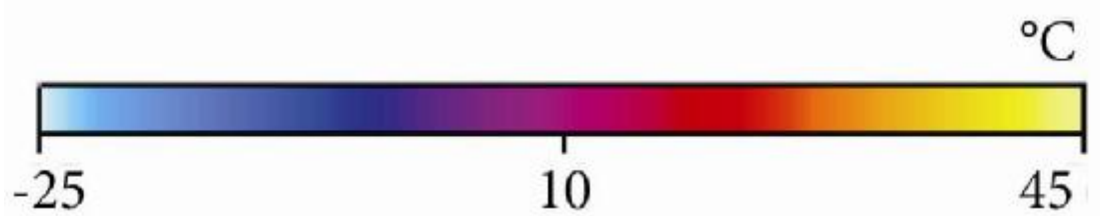

Fig. 3.17: Color scale of daytime land surface temperature map (NASA Earth Observations)

3.2. Analyzing Solar Powered Absorption Refrigeration System

3.2.1. Analysis of Ammonia-Water Absorption Refrigeration System

The laws of mass conservation, the first and second laws of thermodynamics, are used in the analysis of absorption refrigeration system. All components of the system are counted to have an individual control volume and analyzed in accordance with the related principles (Ozgoren et al., 2012). Equations (3.1) and (3.2) should be used for mass conservation where $\dot{m}$ (kg/s) represents mass flow rate and x represents mass concentration of the NH_3.

$$\sum \dot{m}_i - \sum \dot{m}_0 = 0 \tag{3.1}$$

$$\sum (\dot{m} \cdot x)_i - \sum (\dot{m} \cdot x)_0 - 0 \tag{3.2}$$

The first law of thermodynamics for steady stead flow process is presented in Eqs. (3.3). In this equation, h (kJ / kg) is enthalpy, Q (kW) is heat transfer and W (kW) is the shaft power.

$$\sum (\dot{m} \cdot h)_j - \sum (\dot{m} \cdot h)_0 \quad \left[\sum Q_i - \sum Q_0\right] + W = 0 \tag{3.3}$$

Using equations of continuity and first law of thermodynamics, mass and energy conservation are analyzed for each system components. Equations of (3.4), (3.5) and (3.6) are used in order to determine heat transfer capacity of the generator. In these equations, $\dot{m}_3$, $\dot{m}_4$ and $\dot{m}_7$ represent mass flow rates of the rich solutions of heat exchanger, the weak solution returning from the generator and the ammonia vapor exiting from generator respectively. Q_G indicates the heat entered to the generator. Here, h_3, h_4 and h_7 symbolize the enthalpies of the rich solution, the weak solution and ammonia vapor, respectively.

$$\dot{m}_3 - \dot{m}_4 + \dot{m}_7 \tag{3.4}$$

$$\dot{m}_3 x_3 - \dot{m}_4 x_4 + \dot{m}_7 \tag{3.5}$$

$$Q_G = \dot{m}_1 h_1 + \dot{m}_4 h_4 - \dot{m}_3 h_3 \tag{3.6}$$

Equations (3.7), (3.8) and (3.9) are obtained from equations (3.4) and (3.5). Here, f which is stated below is the mass flow rate ratio.

$$f = \frac{\dot{m}_3}{\dot{m}_7} = \frac{1 - x_4}{x_3 - x_4} \tag{3.7}$$

$$\frac{\dot{m}_3}{\dot{m}_7} = \frac{\dot{m}_4}{\dot{m}_7} + 1 \tag{3.8}$$

$$\frac{\dot{m}_4}{\dot{m}_7} = f - 1 \tag{3.9}$$

Equations (3.10) and (3.11) are obtained by applying laws of mass conservation and energy conservation to the condenser. Q_C indicates the amount of heat exiting from the condenser, while $\dot{m}_8$ represents the saturated liquid or compressed liquid ammonia. And, h_7 and h_8 symbolize enthalpy of ammonia entering and exiting the condenser, respectively.

$$\dot{m}_7 - \dot{m}_8 - \dot{m}_{ref} \tag{3.10}$$

$$Q_C = \dot{m}_{ref} (h_8 - h_7) \tag{3.11}$$

Equations (3.1) and (3.3) are applied between inlet and outlet of evaporator to obtain equations (3.12) and (3.13) assuming that there is a steady flow and no shaft power is need. Q_E indicates the heat taken from the cooled space. Here $\dot{m}_9$ represents liquid ammonia after expansion valve, $\dot{m}_{10}$ represents ammonia vapor exiting from evaporator and h_9 and h_{10} symbolize the enthalpy of liquid ammonia and ammonia vapor respectively.

$$\dot{m}_9 = \dot{m}_{10} = \dot{m}_{ref} \tag{3.12}$$

$$Q_E = \dot{m}_{ref} (h_{10} - h_9) \tag{3.13}$$

Equations of (3.14), (3.15) and (3.16) are derived using one dimensional continuity equation and first law thermodynamic to the absorber. Here, $\dot{m}_1$ and $\dot{m}_6$ represent the rich solution that exits in the absorber and the weak solution returning from the generator, respectively. Secondly, h_1 and h_6 symbolize the enthalpy of the rich solution leaving the absorber and the weak solution returning from the generator, respectively. Q_A is the heat taken out from the absorber. Lastly, q_A (kj / kg) is the heat dissipated per unit mass.

$$\dot{m}_1 = \dot{m}_{10} + \dot{m}_6 \tag{3.14}$$

$$Q_A = \dot{m}_1 h_1 - \dot{m}_{10} h_{10} - \dot{m}_6 h_6 \tag{3.15}$$

$$q_A = f \cdot h_1 - h_{10} - (f - 1) \cdot h_6 \tag{3.16}$$

The law of energy conservation applied to the entire system shows that the sum of incoming and out coming heat must be zero. The Eq. (3.17) is obtained when the system is considered to be steady-state process and hence heat losses and the pump work are neglected.

$$Q_C + Q_A - Q_G + Q_E \tag{3.17}$$

The cooling coefficient of performance COP is obtained by ratio of evaporator heat load and generator heat load.

$$COP_{cooling} \quad \frac{Q_E}{Q_G} \quad \frac{\dot{m}_{10}h_{10} - \dot{m}_9 h_9}{\dot{m}_7 h_7 + \dot{m}_1 h_1 - \dot{m}_3 h_3} \tag{3.18}$$

The heating coefficient of performance COP is obtained by ratio of the total heat loads of condenser and absorber with heat load of generator.

$$COP_{heating} = \frac{Q_C + Q_A}{Q_G} = \frac{(\dot{m}_8 h_8 - \dot{m}_7 h_7) + (\dot{m}_1 h_1 - \dot{m}_{10} h_{10} - \dot{m}_6 h_6)}{\dot{m}_7 h_7 + \dot{m}_4 h_4 - \dot{m}_3 h_3} \tag{3.19}$$

While $COP_{heating}$ is arranged according to the Eq. (3.17), it can be written as:

$$COP_{heating} \quad \frac{Q_G + Q_E}{Q_G} \quad 1 + \frac{Q_E}{Q_G} \quad 1 - COP_{cooling} \tag{3.20}$$

The Eq. (3.20) shows $COP_{heating}$ values would be always higher than $COP_{cooling}$ values. The equations (3.21) and (3.22) provide the ideal values of COP. In

these equalities, T_E, T_G and T_C indicate the temperatures of evaporator, generator and condenser, respectively.

$$COP_{ideal\ cooling} = \frac{T_E}{T_G}\left(\frac{T_G - T_C}{T_C - T_E}\right) \tag{3.21}$$

$$COP_{ideal\ heating} = \frac{T_C}{T_G}\left(\frac{T_G - T_E}{T_C - T_E}\right) \tag{3.22}$$

3.2.2. Analysis of the Evacuated Tube Solar Collector

Q_{sol} (kW) is solar radiation received with the solar collector. A is the surface area of solar collector. I (kW/m^2) is the solar radiation.

$Q_{sol\text{-}gen}$ (kW) shows the heat transferred from the solar collector to the generator. η symbolizes the thermal efficiency of solar collector.

$$\eta = \frac{Q_{sol\text{-}gen}}{Q_{sol}} \tag{3.23}$$

Here, τ and α represent coefficient of the transmission and absorption. U is the overall heat transfer coefficient (W/m^{2}K), F is the solar-collector efficiency factor, T_W (°C) and T_A (°C) indicates temperature of the mean water and the ambient air, respectively.

$$Q_{sol} = I \cdot A \tag{3.24}$$

$$Q_{sol\text{-}gen} = F \cdot A[(\tau\alpha)I - U(T_W - T_A)] \tag{3.25}$$

By using Eqs. (3.24) and (3.25), solar collector efficiency can be written as:

$$\eta = F' \cdot (\tau\alpha) - \frac{F' U (T_w - T_a)}{I} \tag{3.26}$$

4. RESULTS AND DISCUSSION

4.1. Hourly Climatic Data

Average values of solar radiation and atmospheric air temperature are obtained by taking the mean hourly values of temperature and solar radiation between 1999 and 2008. These data are taken from a weather station of Turkish State Meteorological Service situated in the province of Mersin (with coordinates of 36.8 latitude and 34.63 longitude at an altitude of 3.4 m). In summery, average values of radiation are obtained according to the hourly average of solar radiation and atmospheric temperature of 10 years.

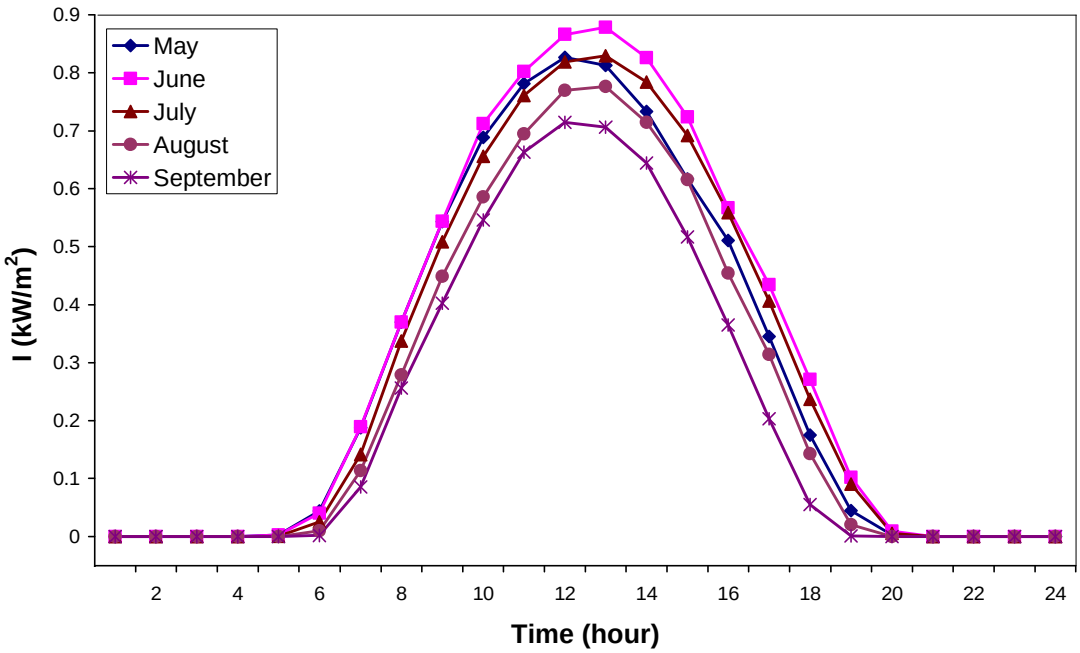

Fig. 4.1: Variations of hourly solar radiation values on the 23rd days of five-months (1999-2008)

Figure 4.1 shows the hourly solar radiation values on the 23rd days of five-months. Solar radiation reaches its highest level at 12:00 a.m. in May and September and at 01:00 p.m. in June, July and August. The highest radiation values are observed in June and the lowest radiation levels are observed in September. The solar radiation is recorded during period of time between 05:00 a.m. and 08:00 p.m. in

May, June, July and between 06:00 a.m. and 07:00 p.m. in August and September. The highest values of solar radiation are obtained as 0.826 kW/m^2 in May, 0.878 kW/m^2 in June, 0.830 kW/m^2 in July, 0.777 kW/m^2 in August and 0.714 kW/m^2 in September.

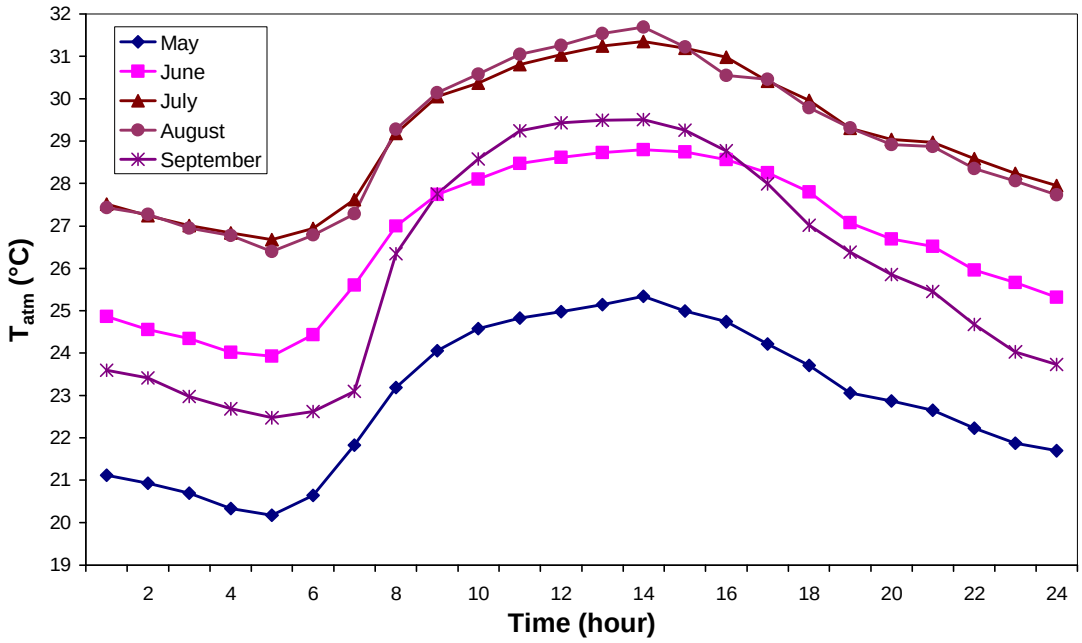

Fig. 4.2: Variations of hourly temperature values on the 23rd days of five-months (1999-2008)

The hourly temperature values observed on the 23rd days of five-months were given in Figure 4.2. Accordingly, the lowest temperatures were observed in May, while the highest temperatures were seen in July and August. The temperature tends to rise with the beginning of radiation at 05:00 a.m. and then, it reaches its highest value at 02:00 p.m. The temperature starts decreasing from 02:00 p.m. until the next day of 05:00 a.m. Temperature values vary from 20.2 °C to 25.3 °C in May, 23.9°C - 28.8 °C in June, 26.7°C -31.4 °C in July, 26.4°C -31.7 °C in August and 22.5°C - 29.5 °C in September.

Figure 4.2 indicates that the highest temperature occurs between 01:00 p.m. and 02:00 p.m. and the highest solar radiation values were recorded between 12:00 a.m. and 01:00 p.m. in the comparison of solar radiation and atmospheric temperature values.

4.2. System Description

System is designed for refrigerating space described in the section 3.1.6. This system consists of absorber, evacuated tube collector, generator, condenser, evaporator, heat exchanger, pump and expansion valves in accordance with solar absorption cooling systems. Thermal storage tank was not used in the present design. Ammonia temperature of generator outlet is 110 °C and evaporation temperature is 10 °C. Condenser and absorber temperatures are assumed to be the same because of cooling from the same source. T_C is 10 °C which is higher than atmospheric air temperature, T_A. That is to say;

$T_C = T_A + 10$ °C

Refrigerated space is located on the fourth floor of the seven-storey building with south and west exposures. There are 2 m×2 m dimensional windows on two exposures of the building. Windows are the most influential factor for heat loads because they directly take solar loads into building. The position and size of windows is important for analysis of the cooling load of building. The thermal loads of building change. Also, the rate thermal loading varies month to month. For example the southern window directly receives sun loads. Heat loads for September are high during the daytime; on the other hand, after the sunset, heat loads for July and August are higher than other months. After the 22nd of June, the southern hemisphere of the world starts to receive sun rays more perpendicular. The thermal loads from southern windows increase with the change of the sun rays angle. This effect is observed with the distributions of Q_E, Q_A, Q_C and Q_G.

4.3. Variation of the Heat Transfer in the Evaporator

The hourly values of Q_E on the 23rd days of five-months are observed in Figure. 4.3. Q_E takes different values during the day. Q_E reaches its highest value at 03:00 pm in August and September; at 04:00 pm in May, June and July. Q_E values range between 2.60 kW and 5.19 kW in May, between 3.80 kW and 8.59 kW in

June, between 4.06 kW and 9.06 kW in July, between 3.88 kW and 9.61 kW in August, between 3.69 kW and 10.27 kW in September.

In five-months, the highest Q_E values are observed in September. It is unexpected result according to solar radiation and temperature values. Especially when solar radiation takes the lowest value on five-months; Q_E values are assumed as also low. But angle of sun ray, position and size of windows cause the highest Q_E values in September. As shown in fig 4.3, the solar radiation affect to cooled space.

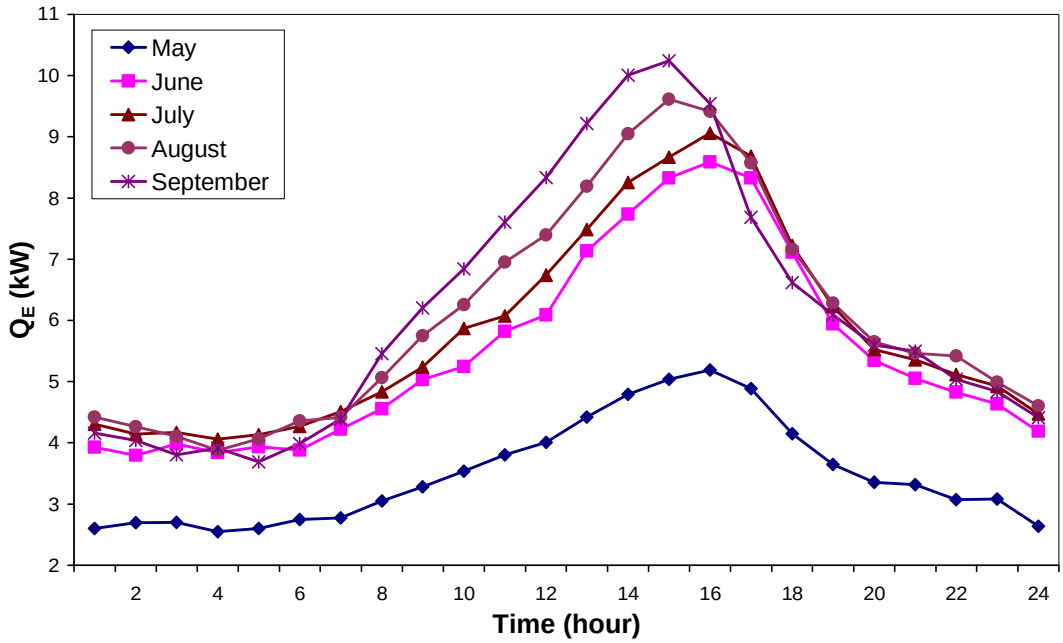

Fig. 4.3: Variations of hourly values of Q_E on the 23rd days of five-months

4.4. Variation of Absorption Refrigeration Machine Efficiency

Figure 4.4 shows hourly values of COP_{IC} for reversible process on the 23rd days of five-months. Here, COP_{IC} designates ideal cooling processes. As seen in this Figure COP value varies according to the magnitude of solar radiation during the day. For ideal cooling case, COP_{IC} changes between 2.18 and 2.92 in May, between 1.83 and 2.35 in June, between 1.62 and 2.03 in July, between 1.59 and 2.06 in August, and between 1.76 and 2.55 in September.

On the other hand, COP_{IH} values of solar powered heating system, for reversible process determined on hourly bases on the 23rd days of five selected months and presented in Figure 4.5. Since the process reversible, COP_{IH} of the solar powered heating system varies between 3.18 and 3.92 in May, between 2.83 and 3.35 in June, between 2.62 and 3.03 in July, between 2.59 and 3.06 in August and between 2.76 and 3.55 in September. Comparison of Figure 4.4 and Figure 4.5 indicates that ideal COP values for heating system are higher throughout all months.

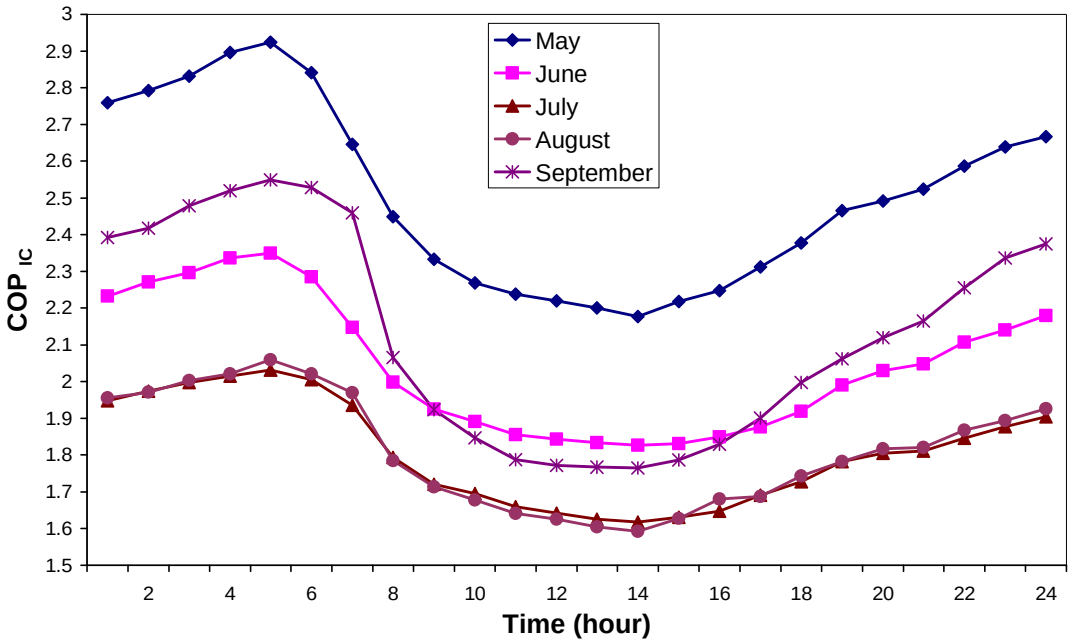

Fig. 4.4: Variations of hourly values of COP_{IH} on the 23rd days of five-months

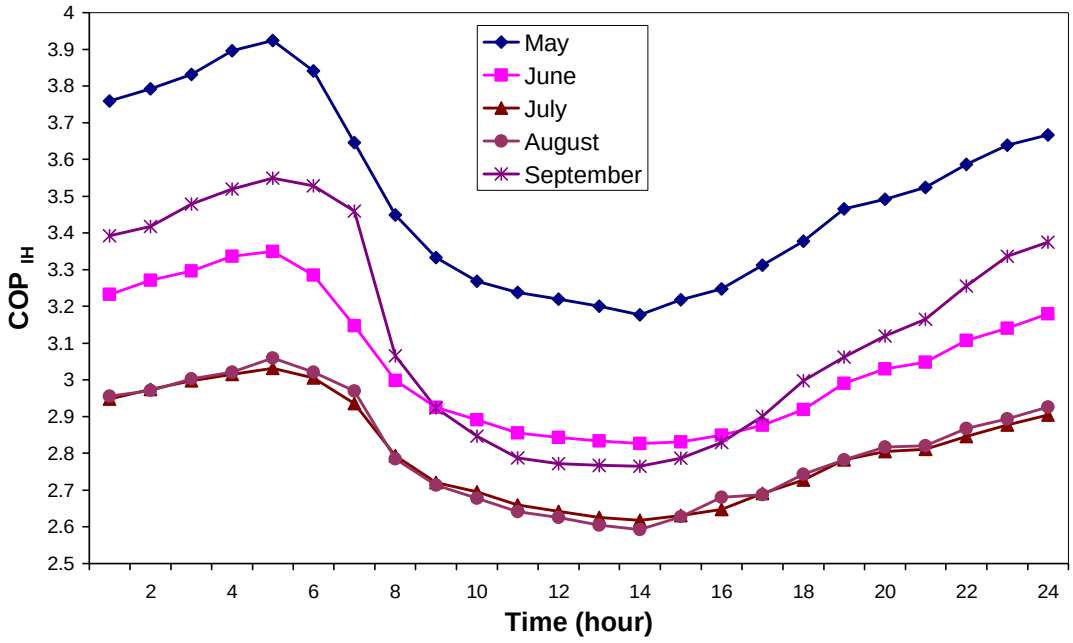

Fig. 4.5: Variations of hourly values of COP $_{IH}$ on the 23rd days of five-months

For 23rd of five selected months COP $_{cooling}$ values of the system considered in this work varies throughout the day as seen in Figure 4.6. COP values change all day. COP $_{cooling}$ values of cooling mode of the system change between 0.46 and 0.49 in May, between 0.43 and 0.47 in June, between 0.41 and 0.45 in July, between 0.41 and 0.45 in August and between 0.41 and 0.45 in September.

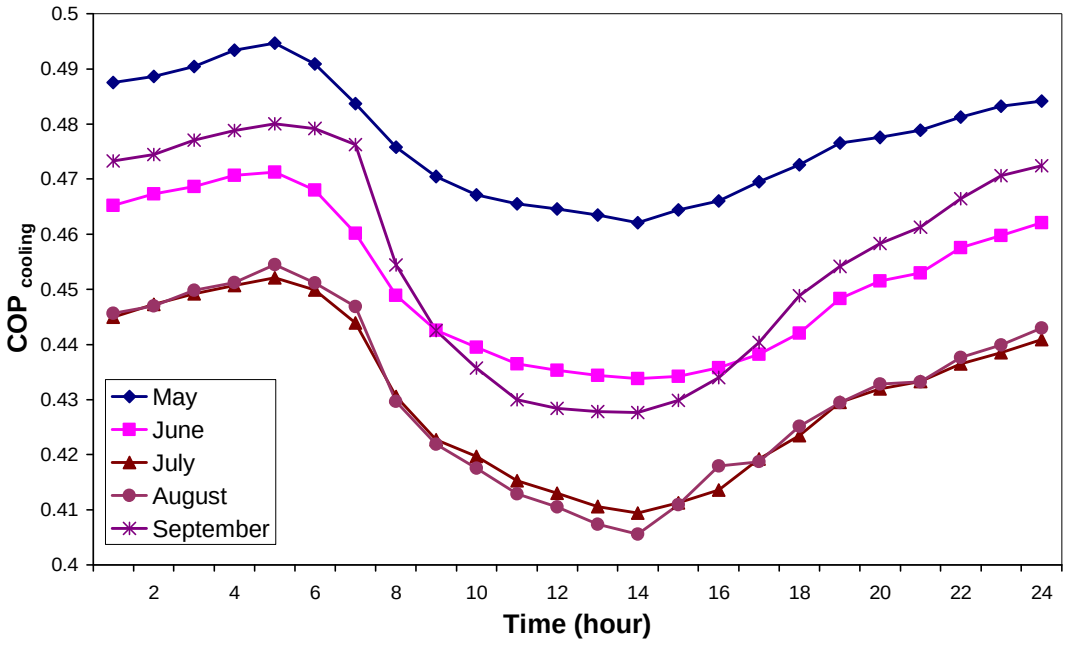

Fig. 4.6: Variations of hourly values of COP $_{cooling}$ on the 23rd days of five-months

Since, we try to present COP values of each component of the main system. Here, COP $_{heating}$ values of heating mode of the main system were examined on the 23rd days of five selected months as presented in Figure 4.6. It is clearly seen that COP $_{heating}$ values of the heating mode of the system change between 1.46 and 1.49 in May, between 1.43 and 1.47 in June, between 1.41 and 1.45 in July, between 1.41 and 1.45 in August and between 1.41 and 1.45 in September.

The highest values of COP $_{heating}$ are seen in May, while the lowest values of COP $_{heating}$ are seen in July and August as indicated in Figure 4.6.

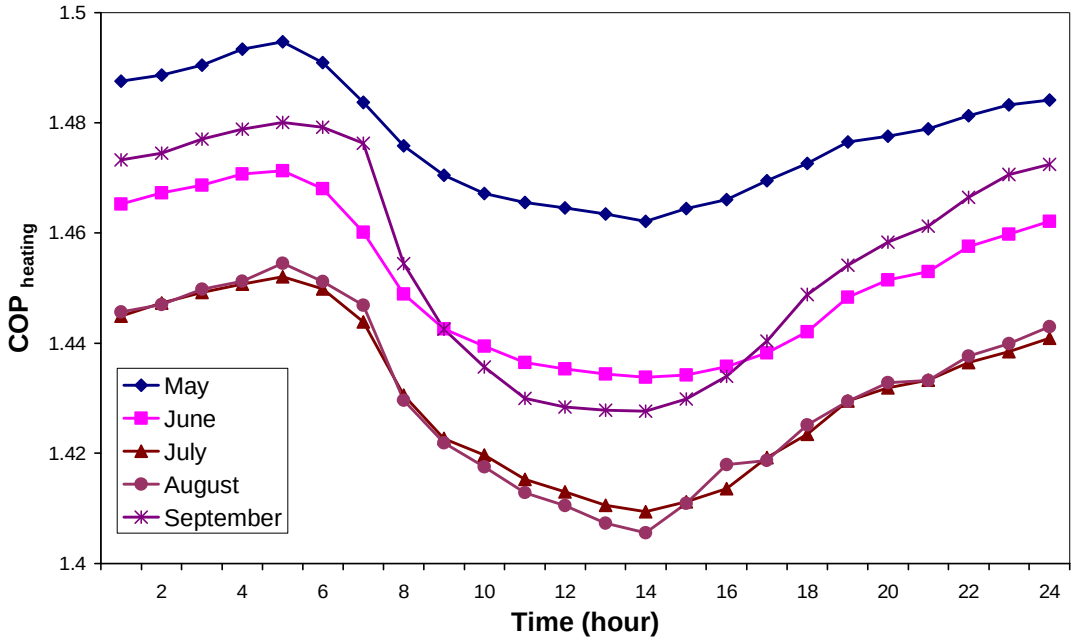

Fig. 4.7: Variations of hourly values of COP $_{heating}$ on the 23rd days of five-months

4.5. Variation of Condenser Capacity

Hourly values of heat transfer, Q_C from the condenser on the 23rd days of five-months reaches its highest value at 03:00 p.m. in August and September, but this highest values of heat transfer take place at 04:00 p.m. in May, June and July as seen in Figure 4.8.Distribution of Q_C show that the values of heat transfer, Q_C vary between 3.13 and 6.31 kW in May, between 4.62 and 10.25 kW in June, between 4.89 and 10.72 kW in July, between 4.67 and 11.37 kW in August and between 4.53 and 12.19 kW in September.

The lowest values of heat transfer from the condenser, Q_C occur at 4:00 a.m. in May, July and August, at 02:00 a.m. in June and at 05:00 a.m. in September. On the other hand, the highest values of heat transfer, Q_C occur at 04:00 p.m. in May, June and July and at 03:00 p.m. in August and September.

In conclusion, the highest values of heat transfer Q_C take place on the 23rd September starting from 07:00 a.m. until 04:00 p.m...

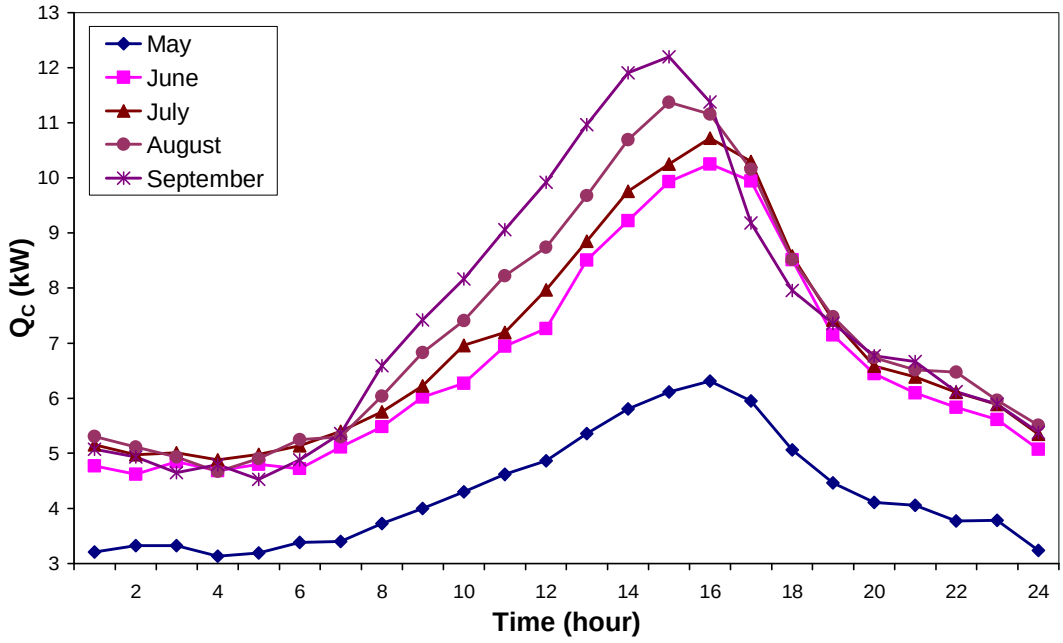

Fig. 4.8: Variation of hourly values of Q_C on the 23rd days of five-months

4.6. Variation of the Heat Transfer in the Generator

One of the important parts of the solar-powered absorption cooling is the generator. The highest rate of heat transfer occurs in this section comparing to other parts. Figure 4.9 shows hourly values of heat transfer, Q_G on the 23rd days of five-months and the changes in Q_G values are observed during the day. Q_G values vary between 5.18 kW and 11.14 kW in May, between 8.13 kW and 19.71 kW in June, between 9.00 kW and 21.90 kW in July, between 8.60 kW and 23.40 kW in August and between 7.69 kW and 23.82 kW in September.

Q_G does not get minimum values at 05:00 a.m. in the calculation of mass, m values with heat transfer of evaporator that dissipated per unit mass, q_E. If q_E was fixed, Q_G would have minimum values at 05:00 a.m. when the atmospheric air temperature takes the lowest value.

The highest values of Q_G are calculated at 03:00 p.m. in September, August, May and at 04:00 p.m. in June and July. On the other hand, the lowest values of Q_G are determined at 04:00 a.m. in May, at 02:00 a.m. in June, at 04:00 a.m. in July and August and at 05:00 a.m. in September.

The highest values of Q_G are observed on the 23rd of September from 08:00 a.m. to 03:00 p.m., and except for these hours, it takes very close values in July and August. Besides, the lowest values are observed in May.

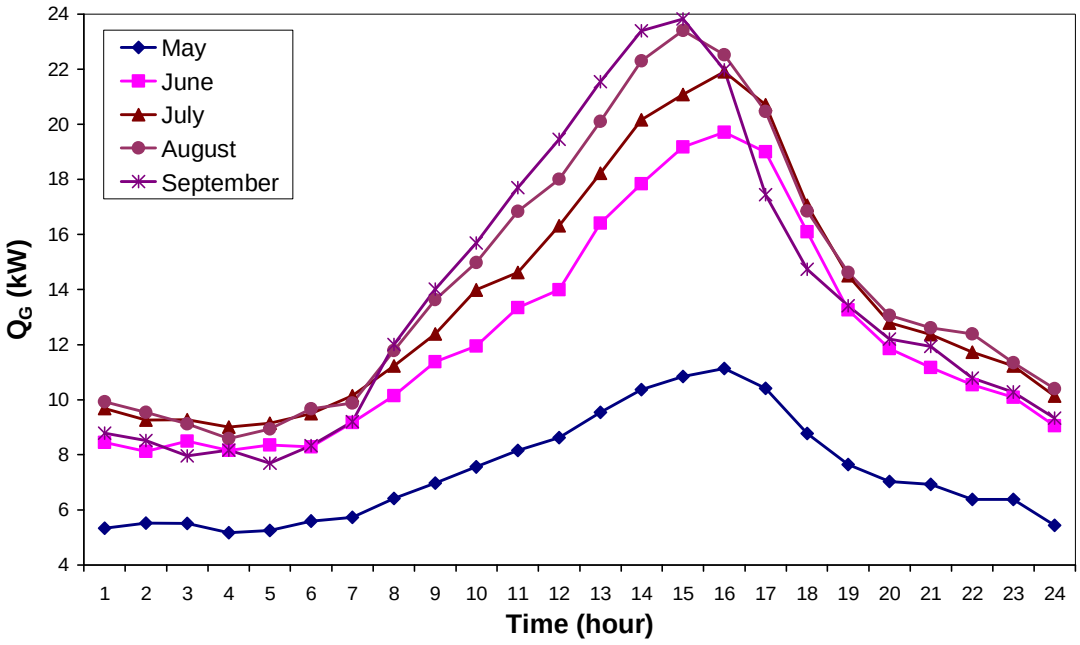

Fig. 4.9: Variation of hourly values of Q_G on the 23rd days of five-months

4.7. Variation of the Heat Transfer in the Absorber

Figure 4.10 shows Q_A hourly values on the 23rd days of five-months. The changes in heat transfer of absorber, Q_A values are observed during the day time. Q_A values vary between 4.59 and 10.02 kW in May, between 7.30 kW and 18.05 kW in June, between 8.18 kW and 20.25 kW July, between 7.80 kW and 21.64 kW in August and between 6.86 kW and 21.86 kW in September.

The highest values of Q_A occur at 04:00 p.m. in May, June, July, August and at 03:00 p.m. in September, while the lowest values of Q_A take place at 04:00 a.m. in May, July, August, at 02:00 a.m. in June and at 05:00 a.m. in September.

The highest values of Q_A are observed on the 23rd of September between 09:00 a.m. and 03:00 p.m., and except for these hours, it takes very close values in July and August, and the lowest values of Q_A are seen in May.

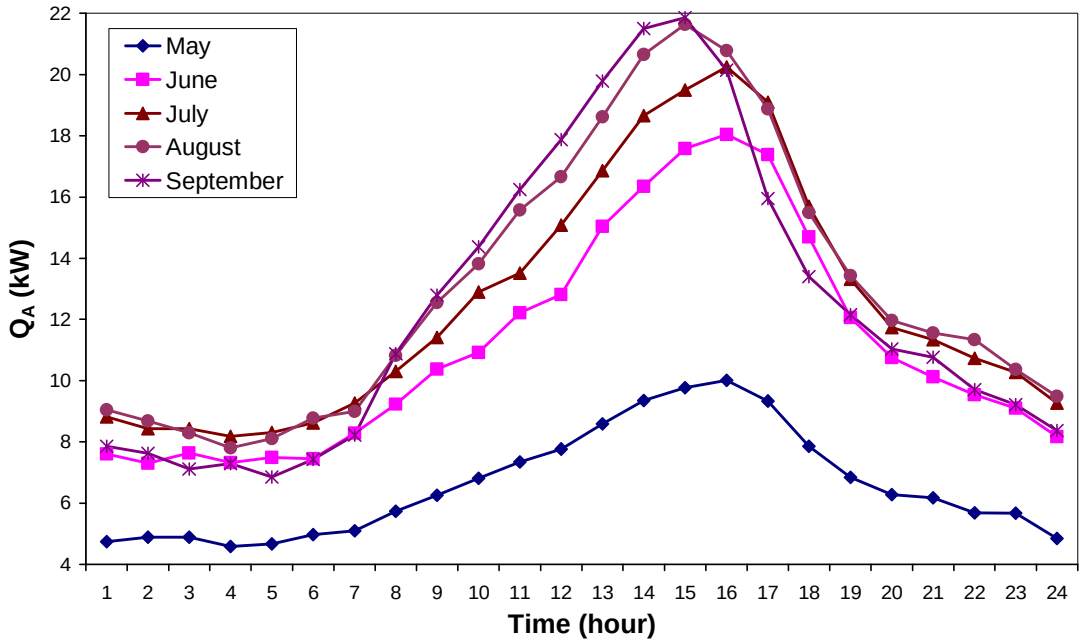

Fig. 4.10: Variation of hourly values of Q_A on the 23rd days of five-months

4.8. Determination of the Required Collector Surface Area

As a result of the calculations, solar collector area that provides hourly cooling requirement throughout specified day of 5 months is calculated in terms of m^2. Table 4.1 shows solar collector areas which are needed in order to provide cooling requirement between 7:00 a.m. and 7:00 p.m. for five-month. The needed collector area can not be calculated at 07:00 pm in May and August and also between 06:00 p.m. and 07:00 p.m. in September since the $Q_{sol\text{-}gen}$ value is zero between these hours. The collector area required for purpose of cooling is calculated as 2229.4 m^2 at 07:00 a.m. on September 23 because the radiation and $Q_{sol\text{-}gen}$ have very small values. For the same reason, the required collector area is calculated as 1119.8 m^2 at 07:00 pm on the 23rd of July and 611.9 m^2 at 07:00 p.m. on the 23rd of June. These results suggest that solar energy utilization is not suitable for each hour of this radiation. Therefore, the cooling process with the solar energy must be evaluated for specific hours. In this study, the cooling process with solar energy is evaluated for hours, in other words, between 8:00 a.m. and 05:00 p.m.

Table 4.1: Solar collector areas needed for providing the necessary cooling capacity between 7:00 a.m. and 7:00 p.m. in throughout five-months

Hour	May	June	July	August	September
7	62.97	96.59	180.98	312.13	2229.42
8	25.80	40.36	49.82	67.20	78.24
9	17.52	28.26	33.17	42.33	50.02
10	14.45	21.83	27.95	34.00	38.85
11	13.52	21.34	24.74	31.50	34.96
12	13.43	20.59	25.46	30.07	35.38
13	15.11	23.78	28.02	33.22	39.68
14	18.43	27.64	32.99	40.41	47.81
15	23.45	34.40	39.62	50.18	62.67
16	30.04	46.66	52.48	68.85	88.35
17	45.65	61.64	72.56	99.14	159.30
18	107.69	96.22	122.29	286.30	-
19	-	611.89	1119.83	-	-

The required collector area for purpose of cooling is given in Figure 4.11 for duration of time between 08:00 a.m. and 05:00 p.m. Accordingly; the required collector areas take the lowest values in May due to the lowest values of the temperatures and the high values of the radiation. The required collector area for cooling is higher in September due to the lowest values of radiation; on the other hand, temperature values are high.

For physical and economic reasons, the optimum value of the required collector area for cooling should be selected for duration of time between 08:00 a.m. and 05:00 p.m. According to the results, the optimum collector area required for cooling requirement is determined as 50 m^2. Table 4.2 shows hourly duration of times when the thermal energy is needed for the generator powered by the solar collector with a collector area of 50 m^2. The shortest time period of solar cooling is observed in September, while the longest time period of solar cooling is determined in May.

Table 4.2: Hourly period of times when the thermal energy is needed for generator powered by the solar collector having a collector area of 50 m^2

Month	Start	Finish
May	07:21 a.m.	05:04 p.m.
June	07:50 a.m.	04:13 p.m.
July	08:00 a.m.	03:48 p.m.
August	08:41 a.m.	02:59 p.m.
September	09:00 a.m.	02:09 p.m.

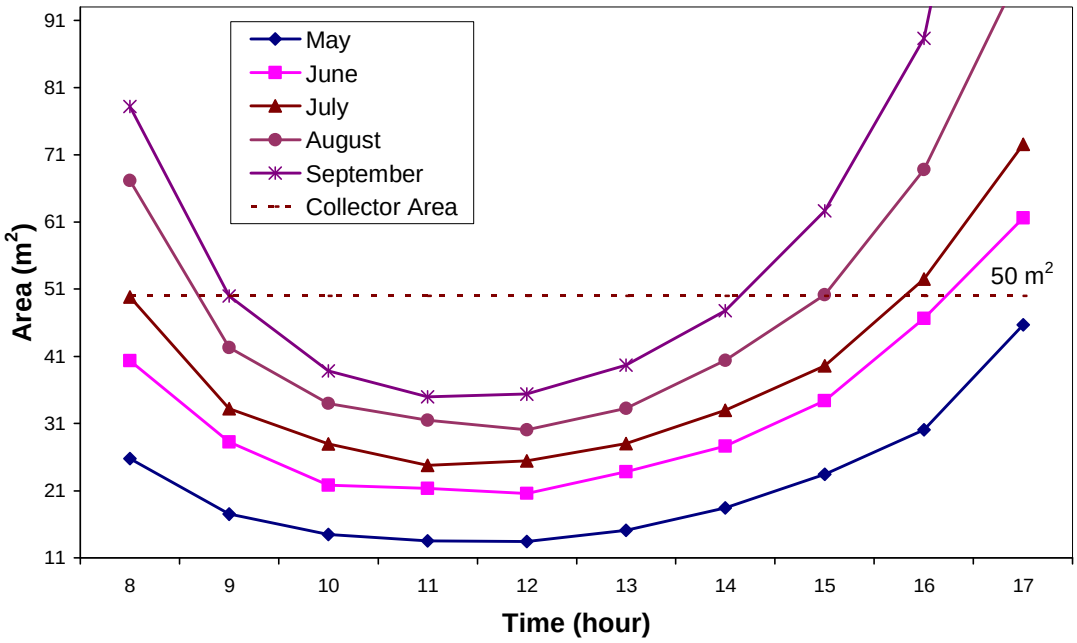

Fig. 4.11: The collector area required for cooling between 08:00 a.m. and 05:00 p.m.

4.9. Variation of the Solar Collector Efficiency, Solar Radiation Production and the Heat Output from Solar Collector

Hourly efficiency of solar collector on the 23rd days of five-months is shown in Figure 4.12. Solar collector efficiency is calculated for solar radiation hours. Solar collector efficiency is directly proportional to the atmospheric temperature and solar radiation. Therefore, solar collector efficiency increases towards the noon time and then it starts to decrease. The solar radiation is more decisive than the atmospheric temperature on the efficiencies of solar collector. Levels of temperatures are lower in May comparing to the value obtained in September but solar radiation level is higher in May comparing to September. Therefore, solar collector efficiency is higher in

May than in September. Between hours ranging from 08:00 a.m. to 05:00 p.m., the value of solar collector efficiency increases from 0.66 to 0.78 in May, from 0.68 to 0.79 in June, from 0.67 to 0.78 in July, from 0.63 to 0.78 in August and finally from 0.54 to 0.77 in September.

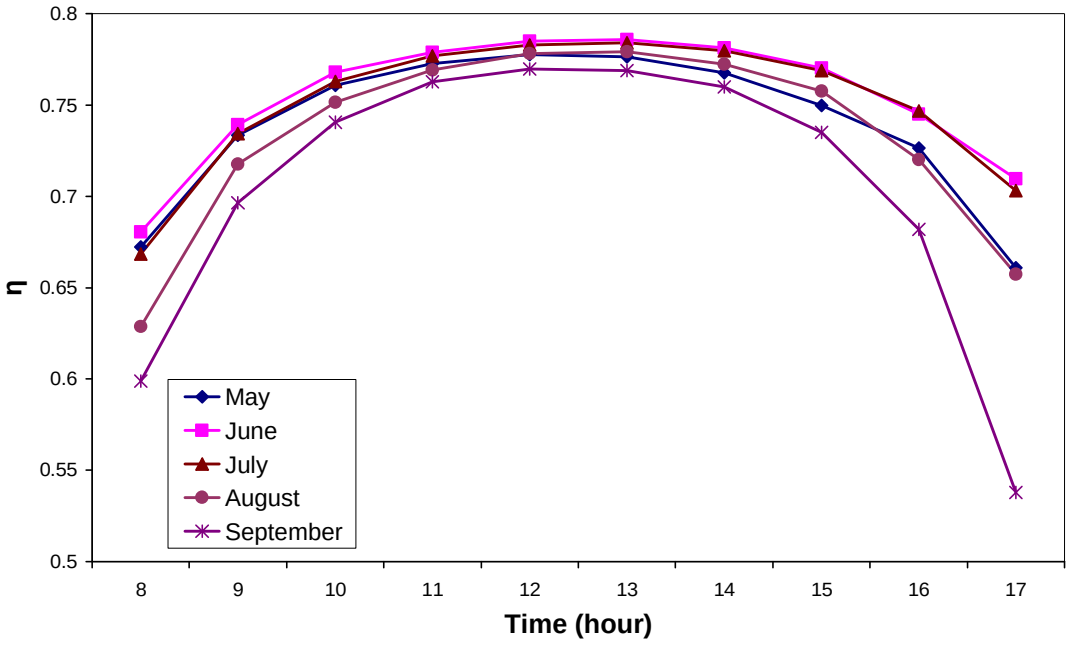

Fig. 4.12: Variation of hourly efficiency of solar collector on the 23rd days of five-months

The total amount of solar heat transfer, Q_{sol} is calculated by multiplying the radiation and the selected collector area. Hourly calculated heat transfer Q_{sol} from radiation on the 23rd days of five months shown in Figure 4.13 demonstrates that there are similarities between distributions of hourly heat received for all months. The highest values of Q_{sol} are observed in June, while the lowest values of Q_{sol} are received in September. Q_{sol} values measured in the hours from 8:00 am to 05:00 pm change from 17.24 kW to 41.31 kW in May, from 18.49 kW to 43.90 kW in June, from 16.86 kW to 41.49 kW in July, from 13.95 kW to 38.83 kW in August and from 10.18 kW to 35.72 kW in September.

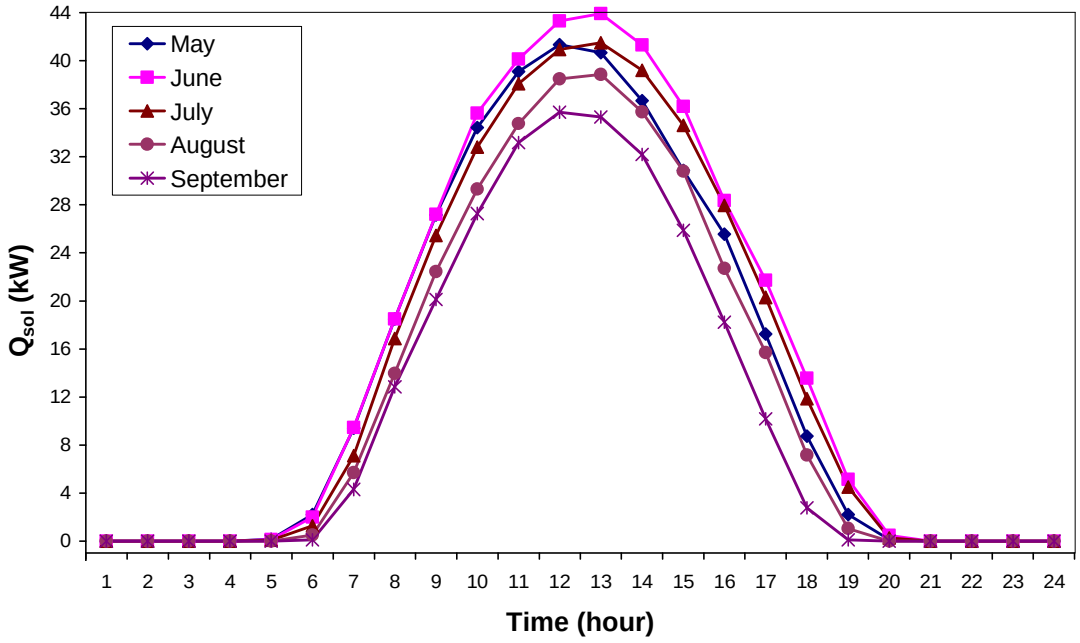

Fig. 4.13: Variation of hourly values of Q_{sol} on the 23rd days of five-months

Efficiency is also considered in the calculation of $Q_{sol-gen}$; therefore, Q_{sol} and $Q_{sol-gen}$ demonstrated similar distributions, but $Q_{sol-gen}$ values are lower than Q_{sol} values and cooling period of $Q_{sol-gen}$ is shorter than cooling period of Q_{sol} (Figure 4.14). $Q_{sol-gen}$ values measured during period of time in the range between 8:00 am and 05:00 pm change from 11.39 kW and 32.13 kW in May, from 12.58 kW and 34.50 kW in June, from 11.27 kW and 32.53 kW in July, from 8.77 kW and 30.25 kW in August, from 5.48 kW and 27.49 kW in September.

4.10. Comparison of the Heat Transfer in the Generator and Heat Output from Solar Collector

In the comparison of the heat transfer in the generator and heat output from the solar collector, the contribution of the solar energy to the required thermal energy for cooling is observed.

The required energy for cooling (Q_G) and solar energy received from the sun ($Q_{sol-gen}$) on the 23rd of May are seen in Figure 4.15. In May, the cooling process can be performed with solar energy between 7:21 a.m. and 05:04 p.m. Cooling

requirement can be achieved by solar energy for all days in terms of storage tank in May because collector area is selected by considering the cooling requirements for a five-month period, so, $Q_{sol-gen}$ values are more than enough.

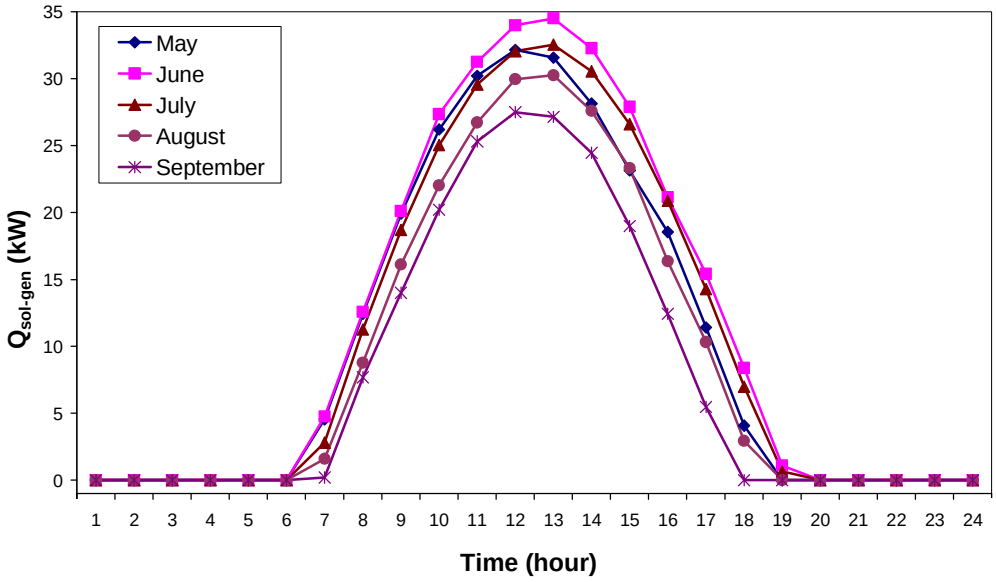

Fig. 4.14: Variation of hourly values of $Q_{sol-gen}$ on the 23rd days of five-months

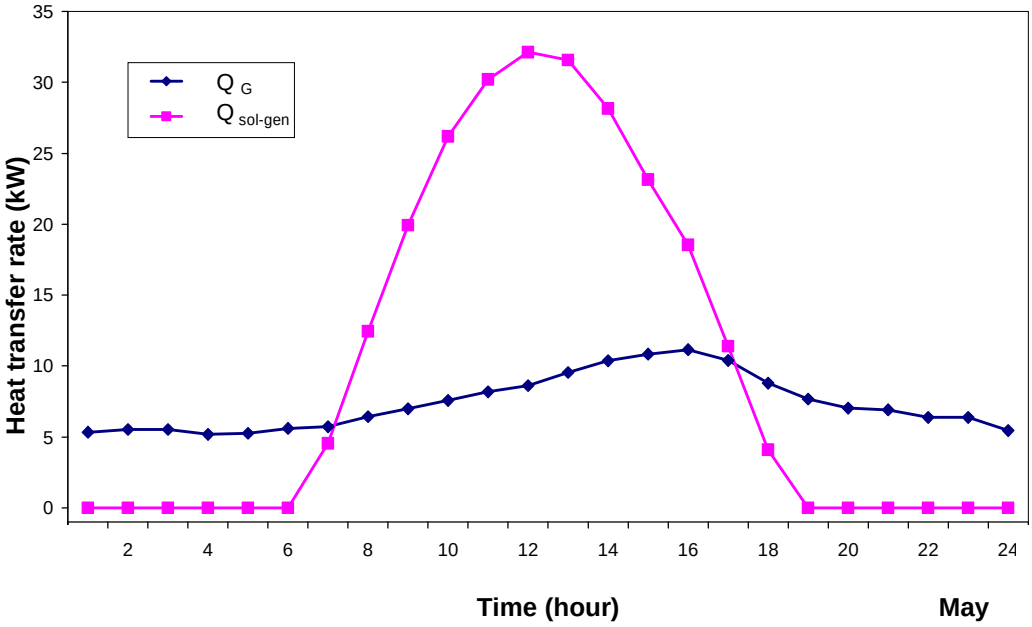

Fig. 4.15: The required energy for cooling requirement (Q_G) and solar energy received from the sun ($Q_{sol-gen}$) on the 23rd of May

Figure 4.16 demonstrates the required energy for cooling purposes (Q_G) and solar energy received from the sun ($Q_{sol-gen}$) on the 23rd of June. In June, the cooling process can be conducted with solar energy between 7:50 a.m. and 04:13 p.m.

Table 4.3: Amount of required additional thermal energy for specified months

Month	Total Q_G (kW)	Total $Q_{sol-gen}$ (kW)	Difference (kW)
May	174.13	242.26	68.13
June	289.83	270.65	-19.18
July	321.65	251.84	-69.80
August	336.02	215.94	-120.08
September	324.00	183.40	-140.60

The highest value of $Q_{sol-gen}$ is seen in June. Q_G value takes the minimum values during four months excluding May. By using storage tank, thermal energy provided with solar energy activates cooling system throughout the day and allows its use similar in May. $Q_{sol-gen}$ is 19.18 kW lower than the required thermal energy for cooling requirement on the 23rd of June (Table 4.3). The system provides cooling process for during day time with an additional source of heating.

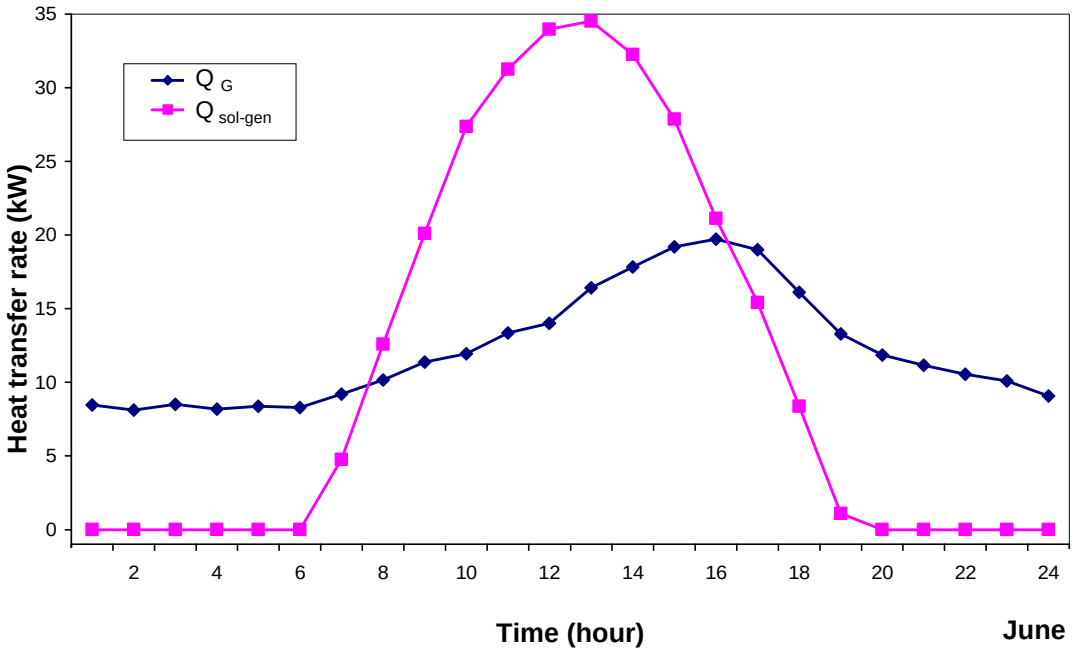

Fig. 4.16: The required energy for cooling (Q_G) and solar energy received from the sun ($Q_{sol-gen}$) on the 23rd of June

Figure 4.17 shows the required energy for cooling (Q_G) and solar energy received from the sun ($Q_{sol-gen}$) on the 23rd of July. In July, the cooling process can be conducted with solar energy between 8:00 am and 03:48 pm. Q_G increases in July, while $Q_{sol-gen}$ decreases. In this case, it becomes more difficult to meet the cooling requirements with the thermal energy provided by solar energy for the entire day. The difference between the required thermal energy and the thermal energy obtained from the sun decreases to 69.80 kW on the 23rd of July. The need for an additional heat source increases in July to provide the necessary cooling for the entire day. Figure 4.18 shows the required energy for cooling requirement (Q_G) and solar energy received from the sun ($Q_{sol-gen}$) on the 23rd of August. In August, the necessary cooling process can be conducted with solar energy between 8:41 am and 02:59 pm.

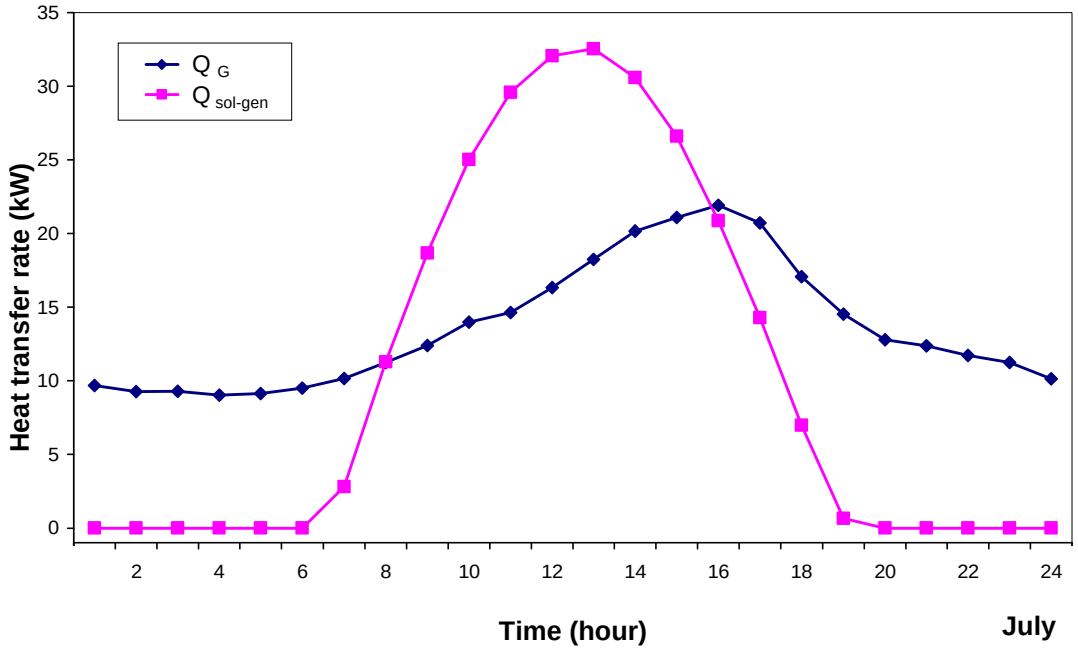

Fig. 4.17: The required energy for cooling (Q_G) and solar energy received from the sun ($Q_{sol-gen}$) on the 23rd of July

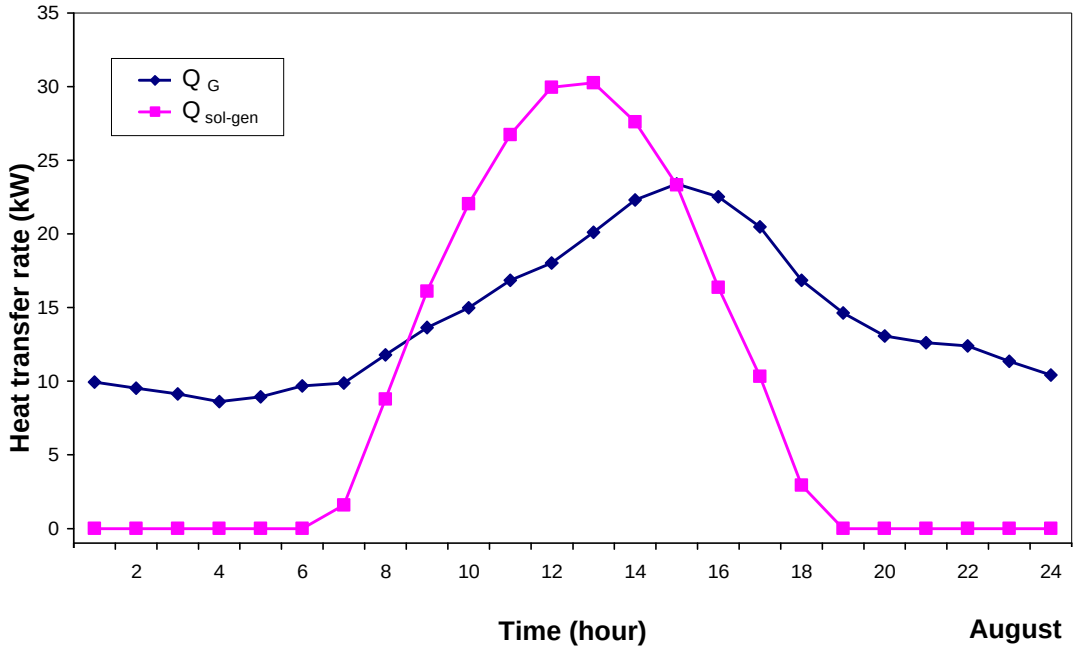

Fig. 4.18: The required energy for the purpose of cooling (Q_G) and solar energy received from the sun ($Q_{sol-gen}$) on the 23rd of August

While Q_G increases in August, $Q_{sol-gen}$ decreases. Naturally, the energy needed from an external heat source increases and additional thermal energy requirements become 120.08 kW. For constant operation of the system all-day, an additional heater must be used as well as the storage tanks.

Figure 4.19 demonstrates the required energy for cooling (Q_G) and solar energy received from the sun ($Q_{sol-gen}$) in September. In September, the cooling process can be conducted with solar energy source between 9:00 am and 02:09 pm.

While Q_G decreases in September, $Q_{sol-gen}$ takes the lowest values of a five-month. The difference between the energy required for cooling requirement and thermal energy from the sun reaches its highest value in September. Naturally, cooling with solar energy can not be achieved during the day even with the storage tank. On the 23rd of September, 140.60 kW of thermal energy must be provided to the system from an additional heat source to ensure, that cooling is conducted for all days.

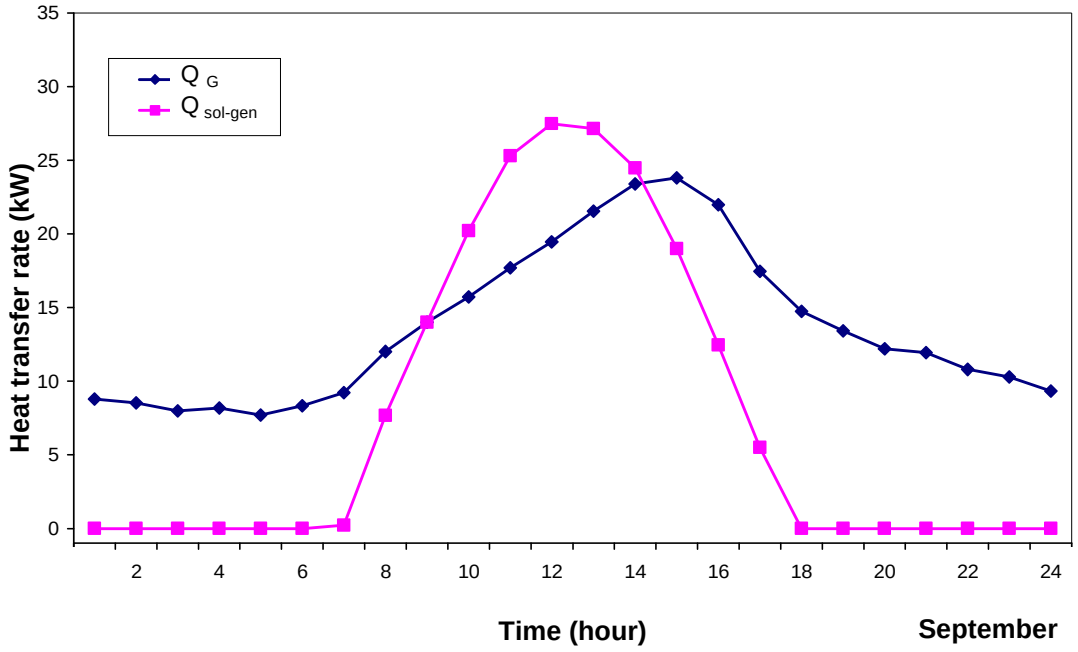

Fig. 4.19: The required energy for cooling (Q_G) and solar energy received from the sun ($Q_{sol-gen}$) on the 23rd of September

5. CONCLUSION

This study investigates the solar-powered absorption cooling system by using hourly temperature and radiation data in Mersin. The obtained results show the benefits and features of using solar energy in the cooling systems. The greatest advantage of these systems is to increase radiation while the requirement for cooling is highest.

The following conclusions can be drawn from the present study:

- Atmospheric air temperature, T_a is the most important factor affecting $COP_{cooling}$. Atmospheric air temperature, T_a is inversely proportional to the value of $COP_{cooling}$.
- COP values vary during the day. $COP_{cooling}$ ranges from 0.46 to 0.49 in May, from 0.43 to 0.47 in June, from 0.41 to 0.45 in July, from 0.40 to 0.45 in August, from 0.43 to 0.48 in September. On the other hand, $COP_{heating}$ values vary between 1.46 and 1.49 in May, between 1.43 and 1.47 in June, between 1.41 and 1.45 in July, between 1.40 and 1.45 in August and between 1.43 and 1.49 in September.
- COP values are also different on the 23rd days of chosen months. The highest values are observed in May, while the lowest values are seen in July and August in presented four Figures of COP.
- The maximum solar efficiency is observed on the 23rd of June at 01:00 p.m. This solar efficiency is calculated as 0.8, while solar radiation is 878 W/m^2.
- Q_G is proportional to the atmospheric air temperature, T_a. On the other hand, Q_G does not get minimum values at 05:00 a.m. for calculating mass, m values with heat transfer of evaporator that dissipated per unit mass, q_E. If q_E was fixed, Q_G would be minimum at 05:00 am when the atmospheric air temperature, T_a takes its lowest value. The highest values of Q_G are measured at 03:00 p.m. in September and August May and at 04:00 p.m. June and July. The lowest values of Q_G are

measured at 04:00 a.m. in May, at 02:00 a.m. in June, at 04:00 a.m. in July and August and at 05:00 a.m. in September.

- The results suggest that solar energy utilization is not suitable for each hour of the radiation. Therefore, the cooling process with the solar energy must be evaluated for specific hours. In this study, the cooling process with solar energy is evaluated for the time period from 8:00 a.m. to 05:00 p.m. The minimum required collector surface areas are found as 13.4 m^2 at 12:00 a.m. on the 23rd of May, 20.6 m^2 at 12:00 a.m. on the 23rd of June, 24.7 m^2 at 11:00 a.m. on the 23rd of July, 30.1 m^2 at 12:00 a.m. on the 23rd of August and 35.0 m^2 at 11:00 a.m. on the 23rd of September. According to the results, the optimum required collector area for cooling is determined as 50 m^2.
- The thermal energy needed for generator can be provided fully for 9 hours, 43 minutes in May; 8 hours, 23 minutes in June; 7 hours, 48 minutes in July; 6 hours, 18 minutes in August and 5 hours and 9 minutes in September.
- The results show that solar-powered absorption cooling system is suitable for use in Mersin.

REFERENCES

AGYENIM, F., KNIGHT, I., RHODES, M., 2010. Design and experimental testing of the performance of an outdoor LiBr/H_2O solar thermal absorption cooling system with a cold store. Solar Energy 84, 735–744

AHACHAD, M., ALMERS, A., MIMET, A.; DRAOUI, A., 2005. Solar-based comparison of adsorption and absorption refrigerating machines. International Journal of Sustainable Energy Vol. 24, No. 4, 199–206

ALI, A.H.H., NOERES, P., POLLERBERG, C., 2008. Performance assessment of an integrated free cooling and solar powered single-effect lithium bromide-water absorption chiller. Solar Energy 82, 1021–1030

ASSILZADEH, F., KALOGIROU, S.A., ALIA, Y., SOPIAN, K., 2005. Simulation and optimization of a LiBr solar absorption cooling system with evacuated tube collectors. Renewable Energy 30, 1143–1159

ATMACA, I., YIGIT, A., 2003. Simulation of solar-powered absorption cooling system. Renewable Energy 28, 1277–1293

BERMEJO, P., PINO, F.J., ROSA, F., 2010. Solar absorption cooling plant in Seville. Solar Energy 84, 1503–1512

BURNS, S.S., GOGGIN, M.S., HINRICHS, D.W., LEE, K.K., 2007. Technical and Economic Assessment of Solar Thermal Absorption Cooling Systems in Small Commercial Buildings. Cogeneration & Distributed Generation Journal, 22: 4, 45 — 56

BÜYÜKALACA, O., YILMAZ, T., 2003. GÜNEŞ ENERJİSİ İLE SOĞUTMA TEKNOLOJİLERİNE GENEL BİR BAKIŞ. ADANA TESİSAT MÜHENDİSLİĞİ Mayıs-Haziran 2003, Sayfa:45-56

ÇOLAK, İ., BAYINDIR, R., DEMİRTAŞ, M., 2008. Türkiye'nin Enerji Geleceği. TÜBAV Bilim Dergisi, Cilt:1, Sayı:2, Sayfa:36-44

EICKER, U., PIETRUSCHKA, D., 2009. Design and performance of solar powered absorption cooling systems in office buildings. Energy and Buildings 41, 81–91

EISSA, M. A. W., 1997. Design of Thermodynamic Charts for Hydrocarbon Mixtures and Influence of Operating Temperatures for Solar Absorption Cooling Cycle. Energy Sources, Part A: Recovery, Utilization, and Environmental Effects, 19: 8, 887 — 900

ERSOY H.K., YALCIN S., YAPICI R., OZGOREN, M., 2007. Performance of a solar ejector cooling-system in the southern region of Turkey. Applied Energy 84, 971–983

FLORIDES, G.A., KALOGIROU, S.A., TASSOU, S.A., WROBEL, L.C., 2002. Modeling, simulation and warming impact assessment of a domestic-size absorption solar cooling system. Applied Thermal Engineering 22, 1313–1325

GENERAL DIRECTORATE OF RENEWABLE ENERGY
http://www.eie.gov.tr/MyCalculator/Default.aspx (accessed 17 June 2014)
http://www.eie.gov.tr/MyCalculator/pages/33.aspx (accessed 17 June 2014)

GOMMED, K., GROSSMAN, G., 2007. Experimental investigation of a liquid desiccant system for solar cooling and dehumidification. Solar Energy 81, 131–138

GROSSMAN, G., 2002. Solar-Powered Systems for Cooling, Dehumidification and Air-Conditioning. Solar Energy Vol. 72, No. 1, pp. 53–62

HVAC-R INDUSTRY EXPORTERS' UNION, 2012. Dünya İklimlendirme Sektörü İthalati Değerlendirme Raporu
http://www.iskid.eu/files/admin/ISIB_ithalat_degerlendirme_raporu.pdf (accessed 17 June 2014)

INTERNATIONAL ENERGY AGENCY, 2014. Key World Energy Statistics.
http://www.iea.org/publications/freepublications/publication/KeyWorld2014.pdf (accessed 15 March 2015)

KABEEL, A.E., 2005. Augmentation of the performance of solar regenerator of open absorption cooling system. Renewable Energy 30, 327–338

KALOGIROU, S., Solar energy engineering: processes and systems - 1st ed. Elsevier Inc., 2009, 760

LECUONA, A., VENTAS, R., VENEGAS, M., ZACARIAS, A., SALGADO, R., 2009. Optimum hot water temperature for absorption solar cooling. Solar Energy 83, 1806–1814

LI, Z.F., SUMATHY, K., 2001. Simulation of a solar absorption air conditioning system. Energy Conversion & Management 42, 313-327

MARC, O., LUCAS, F., SINAMA, F., MONCEYRON, E., 2010. Experimental investigation of a solar cooling absorption system operating without any backup system under tropical climate. Energy and Buildings 42, 774–782

MATEUS, T., OLIVEIRA, A.C., 2009. Energy and economic analysis of an integrated solar absorption cooling and heating system in different building types and climates. Applied Energy 86, 949–957

MAZLOUMI, M., NAGHASHZADEGAN, M., JAVAHERDEH, K., 2008. Simulation of solar lithium bromide–water absorption cooling system with parabolic trough collector. Energy Conversion and Management 49, 2820–2832

MINISTRY OF ENERGY AND NATURAL RESOURCES http://www.enerji.gov.tr/tr-TR/Sayfalar/Gunes (accessed 02 June 2014)

MONNE, C., PALACIN, F., ALONSO, S., 2011. Monitoring and simulation of an existing solar powered absorption cooling system in Zaragoza (Spain). Applied Thermal Engineering Volume 31, Issue 1, Pages 28–35

MUGNIER, D., JAKOB U., 2012. Keeping cool with the sun. International Sustainable Energy Review, Volume 6, Issue 1, 28–30

NASA EARTH OBSERVATIONS (NEO) http://neo.sci.gsfc.nasa.gov/view.php?datasetId=CERES_NETFLUX_M (accessed 18 January 2015) http://neo.sci.gsfc.nasa.gov/view.php?datasetId=MOD11C1_M_LSTDA (accessed 18 January 2015)

OLESEN B.W., “International standards for the indoor environment. Where are we and do they apply worldwide?”

http://www.google.com.tr/url?sa=t&rct=j&q=&esrc=s&source=web&cd=1&ved=0CE0QFjAA&url=http%3A%2F%2Fashrae.org.sg%2FOlesen_International_Standards_indoor_environment.pdf&ei=dlsNUKjYG8fb4QTr7NHfCg&usg=AFQjCNHfPgS2J8LaWgYVFaVfwo-klo1Nhw (accessed 23 July 2012)

ONAN, C., OZKAN, D.B., ERDEM, S., 2010. Exergy analysis of a solar assisted absorption cooling system on an hourly basis in villa applications. Energy, 1-9

OZGOREN, M., BILGILI M., BABAYIGIT, O., 2012. Hourly performance prediction of ammoniaewater solar absorption refrigeration. Applied Thermal Engineering 40, 80-90

PONGTORNKULPANICH, A., THEPA, S., AMORNKITBAMRUNG, M., BUTCHER, C., 2008. Experience with fully operational solar-driven 10-ton LiBr/H_2O single-effect absorption cooling system in Thailand. Renewable Energy 33, 943–949

QU M., YIN H., ARCHER, D.H., 2010. A solar thermal cooling and heating system for a building: Experimental and model based performance analysis and design. Solar Energy 84, 166–182

SANJUAN, C., SOUTULLO, S., HERAS, M.R., 2010. Optimization of a solar cooling system with interior energy storage. Solar Energy 84, 1244–1254

SEVINÇ, K., GÜNGÖR, A., 2012. Güneş Enerjisi Kaynaklı Soğutma Sistemleri ve Bu Alandaki Yeni Uygulamalar. Mühendis ve Makina, cilt 53, sayı 635, s. 59-70

SÖZEN, A., ÖZALP, M., ARCAKLIOĞLU, E., 2004. Prospects for utilization of solar driven ejector-absorption cooling system in Turkey. Applied Thermal Engineering 24, 1019–1035

TURKISH STATE METEOROLOGICAL SERVICE http://www.mgm.gov.tr/veridegerlendirme/gun-derece.aspx?g=merkez&m=33-00 &y=2014&a=05 (accessed 18 January 2015)

TSOUTSOS, T., ALOUMPI, E., GKOUSKOS, Z., KARAGIORGAS, M., 2010. Design of a solar absorption cooling system in a Greek hospital. Energy and Buildings 42, 265–272

U.S. Energy Information Administration, 2013. The International Energy Outlook 2013. http://www.eia.gov/forecasts/archive/ieo13/more_highlights.cfm (accessed 26 March 2015)

WIJEYSUNDERA, N.E., 1999. Simplified Models for Solar-Powered Absorption Cooling Systems. Renewable Energy 16 679-684

_____, 2000. An Irreversible-Thermodynamic Model For Solar-Powered Absorption Cooling Systems. Solar Energy Vol. 68, No. 1, pp. 69–75

YAMANKARADENİZ, R., HORUZ, I., KAYNAKLI, Ö., ÇOŞKUN, S., YAMANKARADENİZ, N., 2009. Soğutma tekniği ve ısı pompası uygulamaları. Dora yayıncılık, Bursa, 690

YANG, R., WANG P.L., 2001. A Simulation Study of Performance Evaluation of Single glazed And Double-Glazed Collectors/Regenerators for an Open-Cycle Absorption Solar Cooling System. Solar Energy Vol. 71, No. 4, pp. 263–268

ZAMBRANO, D., BORDONS C., GARCIA-GABIN W., CAMACHO E.F., 2008. Model development and validation of a solar cooling plant. International journal of refrigeration 31 (2008) 315 – 327

ZHAI, X.Q., WANG, R.Z., 2009. A review for absorption and adsorption solar cooling systems in China. Renewable and Sustainable Energy Reviews 13, 1523–1531

BIOGRAPHY

Altan ÇETİNGÖZ was born in Istanbul, Turkey, at 17.06.1984. He has completed high school education in 2002 at Adile Mermerci Anatolian High School in Istanbul. He received the B.S degree in Mechanical Engineering, Mersin University in 2008.